THE EFFECTS OF EXTRACELLULAR MATRIX COMPLIANCE AND PROTEIN EXPRESSION ON NEURONS

by

MICHELLE L. PREVITERA

A Dissertation submitted to the

Graduate School-New Brunswick

Rutgers, The State University of New Jersey

and The Graduate School of Biomedical Sciences

University of Medicine and Dentistry of New Jersey

in partial fulfillment of the requirements

for the degree of

Doctor of Philosophy

Graduate Program in Cell and Developmental Biology

written under the direction of

Bonnie L. Firestein, Ph.D

and approved by

_____

_____

_____

_____

_____

New Brunswick, New Jersey

January, 2010

ABSTRACT OF THE DISSERTATION

The effects of extracellular matrix compliance and protein expression on neurons

By MICHELLE L. PREVITERA

Dissertation Director:

Bonnie L. Firestein, Ph.D

Extracellular and intracellular cues affect neuronal morphology and contribute to brain diseases, such as schizophrenia, and injury. First, we examined how extracellular cues influence branching parameters of hippocampal neurons. Brain injury or disease can initiate changes in local or global stiffness of brain tissue. While stiffness of the extracellular environment is known to affect the morphology and function of many cell types, little is known about how the dendrites of neurons respond to changes in brain stiffness. We cultured hippocampal neurons on hydrogels composed of polyacrylamide of varying rigidities to mimic the effects of extracellular matrix stiffness on dendrite morphology. At 12 days *in vitro*, dendrite branching was altered by stiffness; i.e. branching peaked in neurons grown on gels of intermediate stiffness (8 kPa). Furthermore, we found that ionotropic glutamate receptors play roles in regulating dendrite morphology. AMPA receptors play a role in dendritc arborization for harder stiffness, $\geq$2kPa, at all distances from the cell body. NMDA receptors play a role in dendritic arborization for a range of rigidities (1-25 kPa), at only proximal and intermediate distances from the cell body. However, a caveat to these studies is that cell adhesion is affected by the rigidity of these substrates. Addressing this caveat is of great

importance because cell density affects dendrite branching. Thus, we also determined whether substrate stiffness plays a critical role in determining dendrite branching independent of cell density. We concluded that substrate stiffness does play a crucial role in determining dendrite branching patterns independent of cell number; however, the density of cells plated on substrates also influences the dendrite branching pattern of neurons. In the second chapter of my thesis, we looked at how intracellular proteins in different sections of the human brain are affected in schizophrenia. By Western blotting, we examined human, postmortem brain samples. NOS1AP protein expression increased in the dorsal lateral prefrontal cortex of patients with schizophrenia and not in the occipital lobe, medial temporal lobe, or cerebellum. Thus, this thesis demonstrates how extracellular and intracellular cues affect disease states, such as brain injury and schizophrenia.

ACKNOWLEDGMENTS

First, I would like to thank my advisor, Dr. Bonnie Firestein, for her support, mentoring, and guidance. She has been an outstanding advisor and I am proud to have worked in her laboratory.

I wish to thank Christopher Langhammer for his computer programs, which were written for my project and Dr. Norell Hadzimichalis for editing this thesis and collaborating with me on Chapter 2. I would like to also thank Dr. Linda Brzustowicz and her laboratory for allowing me to collaborate with them for Chapter 2 of my thesis project.

I would like to thank my committee members, Drs. Li Cai, Renping Zhou, and Christopher Rongo, for their time, guidance, and insight on my thesis project and other projects. I would specifically like to thank Dr. Noshir Langrana, my secondary advisor on the IGERT Training Grant, for his help, guidance, and support on the hydrogel section of my dissertation and for his career advice.

I would like to thank my funding sources, IGERT on Intergratively Engineered Biointerfaces and the Louis Bevier Dissertation Fellowship.

Lastly, I would like to thank my family and friends for their support. Specifically I would like to thank my parents, Maryann and Anthony Previtera, and my husband, Robert Arter, for their unconditional love, support, patience, understanding, and encouragement.

TABLE OF CONTENTS

LISTS OF TABLES

LIST OF ILLUSTRATIONS

INTRODUCTION

GENERAL OVERVIEW

This thesis addresses two questions relating to how the brain functions. The first question is how does extracellular matrix compliance control dendrite branching? This question is answered in two parts. The first part (Chapter 1a) explains the effects of compliance on dendrite branching in cultured hippocampal neurons. The second part (Chapter 1b) addresses a caveat to the way that compliance studies have been conducted. The second question, which is addressed in the second chapter of this thesis, is how does the expression of NOS1AP, a protein that regulates dendrite number, differ in patients diagnosed with schizophrenia compared to normal patients (1)? Together, this thesis explains how a specific protein and the extracellular matrix separately regulate brain function.

Chapter 1: Extracellular Cues

Hippocampus

The hippocampus is thought to play a major role in learning and memory. The hippocampus, being a part of the limbic system, can also regulate emotions and mood. Neurogenesis is a constant phenomenon that occurs in the hippocampus and continues throughout adulthood (2-6). Malfunctions in neurogenesis can lead to physiological disorders, including depression, stress, anxiety, post-traumatic stress disorder, and schizophrenia (7-9). Anti-psychotic drugs have been shown to increase neurogenesis and help prevent psychotic episodes (10-13).

Dendritogenesis

Ramon y Cajal determined that through examination of dendrite morphology, scientists could better elucidate the function of the nervous system. Dendrite morphology is a defining characteristic of neuronal subtypes and is diverse in the brain (14). Targeting and pruning of growing dendrites are also important in defining neuronal circuitry. Defects in dendritogenesis can result in cognitive and psychological disorders, such as autism, Rett's syndrome, Down's syndrome, and schizophrenia (15, 16).

Dendritogenesis is a multi-stage process and can be observed using cultured dissociated rat hippocampal neurons. As described by Banker and colleagues, neurons form lamellipodia that adhere to the plate at initial plating (stage 1) (17). Next, primary dendrites extend from the cell body from 1 day *in vitro* (DIV) until at least 10 DIV (stages 2–4) (17). Higher order branches then extend from the primary dendrites from 6 DIV until 12 DIV (stage 4) (17, 18). Soonafter, a maturation process occurs from 12 DIV until 21 DIV by permitting spine formation and pruning of some of the primary and secondary dendrites (stage 5) (17). It is important to note that the DIV when these stages occur is highly dependent on culture conditions.

Regulation of dendrite branching is controlled by intrinsic and extrinsic factors. For example, BDNF, neurotrophin-3, NGF, agrin, and reelin are extracellular proteins that regulate dendrite branching (19-27). PSD-95, cypin, and snapin are intrinsic factors that regulate dendrite branching in the hippocampus, and these proteins have been studied extensively in the Firestein laboratory (18, 28, 29). However, proteins are not the only factors to regulate dendrite branching; extracellular matrix compliance has also been shown to regulate dendrite branching (30-33). In the first chapter of this thesis, we examine how extracellular matrix compliance, or stiffness, affects dendrite branching

using hydrogels, and we identify a mechanism by which dendrite branching is regulated on hydrogels. Furthermore, we address caveats to the use of hydrogels in cellular studies.

Dendrite Branching *in vivo*

Patterning of dendrites *in vivo* is important for proper connectivity. Neuronal population is diverse in shape and size (14). The shape and size of a neuron are important for creating the proper local circuit. Improper branching has been observed in patients with cognitive and neurological disorders as well as in neurodegenerative diseases.

There is a loss of dendrite number, length, and branching in patients or animal models with neurological diseases/disorders. For example, patients with autism, a cognitive disorder affecting social and communication skills, have fewer neuronal basal and apical branches compared to control patients.(15, 34). Patients with Rett syndrome, a cognitive disorder that results in developmental reversals, have fewer neuronal basal branches compared to control patietns (15, 35). Patients with epilepsy, a brain disorder resulting in spontaneous seizures, have fewer neuronal proximal branches compared to control patients (36). Patients with Alzheimer's disease, a neurodegenerative disease that results in a severe loss of memory and thinking, have fewer dendrite number compared to control patients (37). Moreover, patients diagnosed with Parkinson's disease, a neurodegenerative disease of the central nervous system that impairs motor function, have fewer and short dendrites (38-41). Moreover, amyotrophic lateral sclerosis mouse models, a neurodegenerative disease affecting voluntary motor control, have fewer and shorter dendrites (42). These studies show that dendrite number and patterning is altered in patients and models with neurological disorders and diseases.

Hydrogels

Currently, there are technical limitations as to how biologists study neuronal morphology. Neurons are plated on glass coverslips, which do not represent physiological conditions because glass is approximately 500 times stiffer than an adult brain (30). Plating neurons on softer substrates would be more physiologically relevant.

Hydrogels can be designed to mimic shear moduli of native brain tissue, which is 300 $\pm$ 100 Pa, unlike glass, which is in the MPa to GPa range (30). Hydrogels can also be designed to mimic changes in brain stiffness due to injury or disease (43-49). Hydrogels can be composed of naturally occurring materials, such as agarose, fibrin, and collagen or of synthetic materials, such as polyacrylamide (PA).

There are advantages and disadvantages to both materials. On the one hand, naturally occurring materials are more biocompatible and less toxic. On the other hand, PA gels have certain beneficial properties for mechanical studies. First, PA gels are inert and must be functionalized by covalently linking adhesive ligands to the gel surface (30, 50). This property allows one to control which proteins are attached, while attaching them equivalently on soft and hard gels (30). Furthermore, the rigidity of PA gels can be altered by varying only the percentage of the cross-linking agent, *N*, *N* 8-methylene-bis-acrylamide (bis), and not total monomer concentration (acrylamide), ensuring that gel chemistry and topography are independent of stiffness (30, 51-53). To increase the stiffness of collagen or fibrin gels, total protein concentration must be increased, potentially changing the gel's pore size and available adhesion sites (52, 54).

To examine dendritic branching, we took a biomechanistic approach by using PA hydrogels to control the stiffness that cultured neurons were grown on. The ultimate goals of these experiments were to evaluate the effects of stiffness on dendrite branching and to

identify the mechanisms affecting branching (Chapters 1). Furthermore, compliance studies have a caveat: soft and hard matrices have different cell adhesion properties, which may affect neuronal morphology (30, 32, 51). We address this caveat to observe if our dendrite branching data are affected by cell density.

The PA gel will serve as a model to understand how branching occurs under physiological conditions while also serving as a model to understand disease and injury conditions that change brain rigidity.

Chapter 2: Intracellular Cues

Nitric oxide (NO) is highly reactive gas involved in local cell signaling. NO rapidly diffuses through cell membranes and acts locally because of its short lifetime in the extracellular matrix. NO can quickly convert to nitrates or nitrites by reacting with oxygen in the extracellular matrix. NO is produced from L-arginine by nitric oxide synthase (NOS).

NO has been found to signal in the central and peripheral nervous systems (55-57). It performs post-translational covalent modification of proteins for signaling. In addition, excessive NO has been shown to cause neurodegenerative diseases, such as Parkinson's disease (58). Moreover, NO has been shown to play a role in stress and depression (59).

NOS1, an isoform of nNOS (neuronal nitric oxide synthase), is predominately expressed in neurons (60). NOS1 knockout mice have demonstrated behavioral and signaling abnormalities (61). NMDA receptors (NMDAR) bind intracellularly to post-synaptic density 95 (PSD-95), and PSD-95 binds to nNOS (62). Stimulation of NMDAR

leads to the influx of calcium ions into the neuron (63). This influx of extracellular calcium then leads to the activation of nNOS and the synthesis of NO (**Figure 1**) (55).

The N-terminal PDZ domain of NOS1 binds to adaptor proteins for targeting of NOS1 in cell signaling (64, 65). The nNOS adaptor protein (NOS1AP and also known as CAPON) regulates NOS1 localization (66). NOS1AP can regulate NOS1 signaling by binding to proteins, such as Dexras1, to induce signaling or by competing with proteins, such as PSD-95, to inhibit signaling (66, 67).

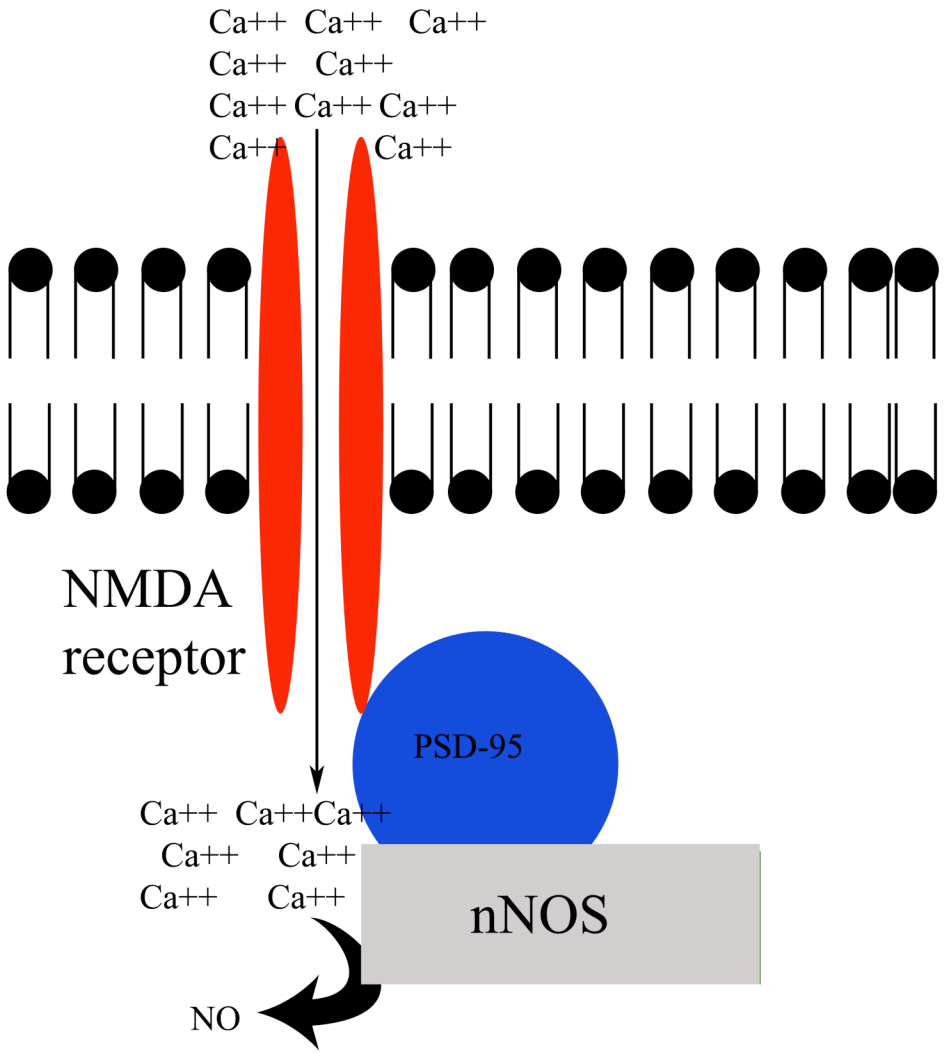

Figure 1. Coupling of NMDAR and nNOS.

Single nucleotide polymorphisms (SNPs) in NOS1AP are associated with schizophrenia (68). Schizophrenia is a serious psychological disorder with a genetic component affecting about ~1% of the population (69). Two human isoforms of NOS1AP have been discovered, a short form and a long form (70). Previous reports document increased expression of the short isoform of NOS1AP in the dorsal lateral prefrontal cortex (DLPFC) for patients diagnosed with schizophrenia (70). Moreover, specific SNP alleles associate with the disease and increased NOS1AP expression (70). We observe whether NOS1AP is differentially expressed in distinct regions of the brain in patients diagnosed with schizophrenia (Chapter 2). This thesis work was performed in collaboration with Dr. Norell Hadzimichalis and the laboratory of Dr. Linda Brzustowicz.

Chapter 1: Extracellular Cues

CHAPTER 1a: Regulation of dendrite arborization by substrate stiffness is mediated by glutamate receptors.

INTRODUCTION

Numerous studies have focused on understanding the physiological, physical, and chemical consequences of traumatic brain injury. On a global level, when brain injury occurs, there is an increase in brain stiffness, which can be due to scarring or intracranial pressure (43, 45-49). On a local or cellular level, injury to astrocytes causes a decrease in astrocyte stiffness (44). However, little is known about the effects of changes in brain stiffness on neuronal morphology. In this study, we observed how increasing substrate stiffness affects dendrite branching in cultured hippocampal neurons. Moreover, we uncover receptors responsible for changes in dendrite branching due to varying extracellular matrix compliances.

The hippocampus is responsible for learning and memory and is often damaged during traumatic brain injury. Aberrant dendrite morphology has also been observed in hippocampal neurons in patients suffering from neurological disorders (15). *In vitro* studies, using fibronectin or collagen as a ligand or matrix, showed changes in neurite outgrowth with changes in extracellular matrix stiffness (33, 71). The increases in outgrowth seen on these gels may be due to altered gel pore size, which subsequently increases available adhesion sites for neurites (52, 54). Furthermore, increasing collagen concentration to increase gel stiffness may in itself contribute to changes in neurite outgrowth since more collagen is available for neurite binding (72).

Utilizing polyacrylamide (PA) gels eliminates the effects of varying ligand concentration, gel pore size, and other variables on neurite outgrowth. PA gels are inert and must be functionalized by covalent linkage of adhesive ligands to the gel surface (30, 50, 52, 73). This property allows for control of protein attachment and for the possibility

of attaching proteins in equal amounts on soft and hard gels (30, 51, 52). Moreover, non-ligand based gel functionalization can be used, such as poly-D-lysine coating, to allow neurons to adhere onto gels without the activation of ligands. Furthermore, gel chemistry is independent of stiffness because the stiffness of PA gels can be altered by varying the percentage of crosslinking agent (*N*, *N* 8-methylene-bis-acrylamide) and not total monomer concentration (acrylamide) (30, 51, 52).

In this study, we use hippocampal neurons to observe how stiffness affects dendrite patterning and to elucidate a possible mechanism for mechanosensing by neurons. Hippocampal neurons were plated onto PA gels and treated with DL-2-amino-5-phosphonovalerate acid (APV) or 6-cyano-7-nitroquinoxaline-2,3-dione (CNQX), NMDA and AMPA receptor antagonists, respectively. We then assessed whether these receptors contribute to the alterations in dendritic arborization seen on gels of differing stiffnesses. We found that dendrite branching peaks when the neurons grow on gels of intermediate stiffness (8 kPa). We also found that blocking NMDA and AMPA receptors alters the changes in dendrite branching at different distances from the soma seen when the neurons are plated on gels of different rigidities.

MATERIALS AND METHODS

PA gel preparation

PA gels were made as previously described with modification (30, 51). Briefly, gels were composed of 7.5% acrylamide and 0.02, 0.03, 0.1, or 0.6% *N*, *N8*-methylene-bis-acrylamide (bis) for varying rigidities. Acrylamide and bis were degassed for 30 mins by dessication. Gels were polymerized on 12 mm round glass coverslips with 0.3% N, N, N9, N9-tetramethylethylenediamine and 0.1% ammonium persulfate. Next, gels were functionalized by UV irradiation of Sulfo-SANPAH. Gels were placed in 12 well plates and coated with Poly-D-Lysine (0.2 mg/ml) for 30-60 minutes at 37°C. Gels were equilibrated in 12 well plates with Neurobasal media (Invitrogen) supplemented with B27, penicillin, streptomycin, and L-glutamine with beta-mercaptoethanol or Glutamax.

Compression testing

Cylindrical gels were made and placed in 50 mM HEPES, pH 8.2, for 16 – 48 hours. Forces were measured with a Mark-10 EG 025 series digital force gauge with flat adaptor (Johnson Scales, West Calwell NJ). (Force/sample radius) vs. (displacement/sample height) was graphed in Excel to determine the slope, taken as Young's modulus. Only the linear portion of the graph was used to determine the slope. The experiment was performed in triplicate.

Rheology

Gel stiffnesses of 0.02, 0.1, and 0.6% gels were measured by rheometry in one session. The dynamic shear moduli of polyacrylamide gels were quantified to describe the elastic

properties of the gels using an SR-2000 rheometer (Rheometrics Inc., Piscataway, NJ). Polyacrylamide (0.5 ml) was polymerized between 25 mm parallel plates, resulting in an approximate sample thickness of 1 mm. The shear modulus, corresponding to the elastic resistance of the gels, was determined from the shear stress in phase with an oscillatory shear strain of 2% amplitude at a frequency of 10 rad/s. Strain sweep was also determined at a low strain. Polyacyrlamide does not stiffen with strain, and thus, it is assumed that the G' does not change with changes in strain. Shear modulus was converted to Young's modulus to maintain consistency. Poisson's ratio was taken to be 0.5 because the gels are assumed to be incompressible (Equ. 1).

Equation 1: $E=2G'(1+\nu)$

Primary neuronal culture

Neuronal cultures were prepared from hippocampi of E18 rat embryos as we have previously described (18, 29, 74). The hippocampi were dissociated by mechanical trituration. Cells were plated onto the gels or glass at a density of 60,000 cells/cm^2. Cultures were maintained in Neurobasal media supplemented with B27, penicillin, streptomycin, and L-glutamine plus 8.5 mM 2-mercaptoethanol or Glutamax.

Transfection

For dendrite visualization, neurons were transfected with cDNA encoding GFP using a modified calcium phosphate method on DIV 7 or 8. (75-78). Briefly, 500 µl of 2X HeBs (pH 7.1; 274 mM NaCl, 10 mM KCl, 1.4 mM $Na_2HPO_4 \cdot 7H_2O$, 15 mM dextrose, and 42 mM Hepes) was mixed with 500 µl of a solution containing 15 µg of DNA and 0.25 mM

$CaCl_2$. This mixture was incubated for 25 minutes in the dark at RT. Next, 60 µl of the mixture was dropped into each well containing Neurobasal media supplemented with B27 only. The solution was allowed to precipitate for 30-45 minutes in the incubator. Media containing precipitate was removed and replaced with the original supplemented Neurobasal media plus 15% fresh supplemented Neurobasal media.

Pharmacological treatment

For antagonist treatment, neurons were treated with 50 µM DL-2-amino-5-phosphonovalerate acid (APV) or 10 µM 6-cyano-7-nitroquinoxaline-2,3-dione (CNQX) at 10 DIV for 24 hours as previously described (29). On DIV 12, neurons were fixed with 4% paraformaldehyde in phosphate-buffered saline for 30 minutes at 37°C.

Dendrite analysis and imaging

To prevent bias by the experimenter, only GFP transfected neurons were imaged. No neurons were excluded from imaging. Neurons were imaged in the GFP channel at 200x using an Olympus Optical IX50 microscope (Tokyo, Japan) with a Cooke Sensicam CCD cooled camera, fluorescence imaging system and ImagePro software (MediaCybernetics, Silver Spring, MD). Neuronal morphology was digitized in three stages based on these initial images. In the first stage, the semi-automated tools available through the NeuronJ plugin to ImageJ (NIH, Bethesda MD) were used to define coordinates of all dendrites in the x-y plane. All neurites were counted. In the second stage, NeuronStudio was used to define the pattern of connectivity between dendrites. These two steps fully determine the structure of each cell's dendritic arbor and encode it in a digital format. Custom scripts written in MATLAB (MathWorks, Natick, MA) were used to transfer the data from NeuronJ to NeuronStudio. Using these digitized dendritic arbors, a second set of

MATLAB scripts were then used to analyze data and extract the following metrics: number of primary dendrites, number of secondary dendrites, number of branch points per cell, number of terminal dendrite points per cell, and Sholl analysis performed with a 9.3 μm ring interval. Afterward, data were transferred to Excel to facilitate statistical analysis. The experimenter was blinded to condition during all data analyses. Dendrites less than 3 μm in length were not counted. Dendrites were labeled as proximal (1-63 μm from the cell body), intermediate (64-123 μm from the cell body) and distal (124-183 μm from the cell body). Statistics were not performed for intersections >183 μm from the cell body.

Statistics

GraphPad Instat Software (San Diego, CA) was used to calculate statistics. Statistical analysis was performed using ANOVA followed by the appropriate *post hoc* test.

RESULTS

Increasing *N8*-methylene-bis-acrylamide (bis):acrylamide

Gel stiffness was chosen based on previously published literature (30, 51). Stiffness was measured in Young's modulus by compression testing. All data for this work and published work were converted to Young's moduli (Equ. 1). The Young's moduli values increased with increasing bis:acrylamide concentration. Young's moduli of the 0.02, 0.1, and 0.6% gels (% bis) were measured by rheology. 0.03% gels were not tested because measurements were previously published to be approximately 2 kPa (51). 0.1% gels were a positive control. Again, the Young's modulus value for rheology significantly increased with increasing bis:acrylamide concentration (**Figure 2**). The stiffness of these gels, based on rheology and compression testing, are approximately 1, 2, 8, and 25 kPa for 0.02, 0.03, 0.1, and 0.6 % gels, which are within the range of rigidities appearing in previously published data (**Figure 2**) (30, 51). There is no significance between rheology and compression data.

Our data agree with previously published results (30, 51). The positive control for compression testing, 0.1% gel, was measured at approximately 8 kPa which is within the range of rigidities appearing in previously published data (**Figure 2**) (51). By rheology, Georges et al. measured 0.01% and 0.3% gels to be approximately 600 Pa and 18 kPa, respectively, which fits in with our data (30). Also by rheology, Yeung et al. measured 0.01, 0.03, 0.1 and 0.3% gels to be approximately 600 Pa, 2 kPa, 8 kPa, and 18 kPa respectively (51).

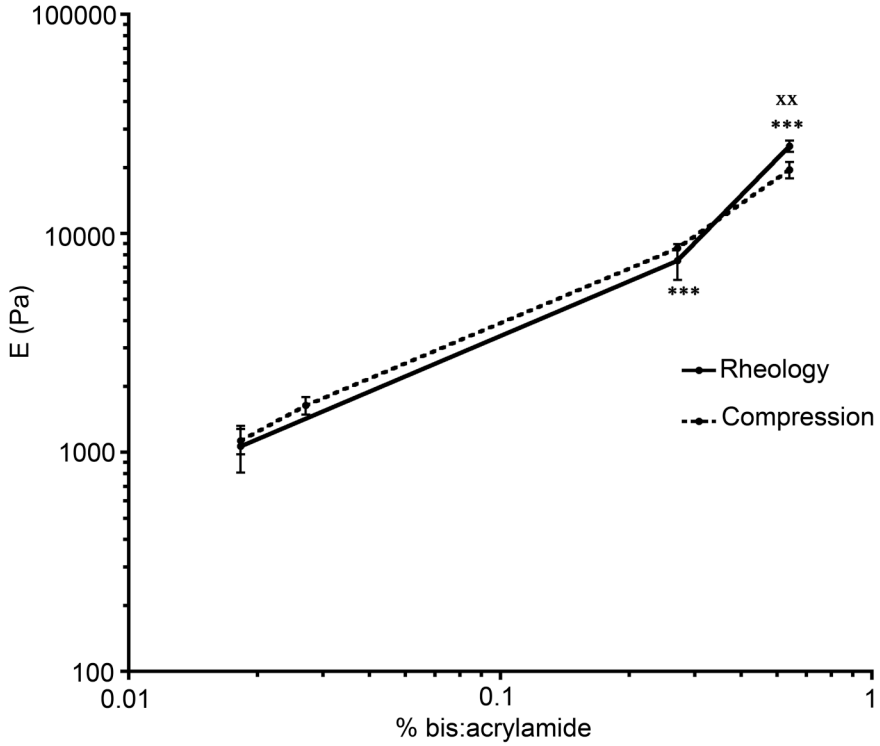

Figure 2. Increase in N, N8-methylene-bis-acrylamide (bis) concentration results in an increase in gel stiffness. As bis concentration increases, gel stiffness increases, as expected (51). The values for the compression experiments are an average of the values measured from three experimental trials (mean + SEM) (dotted line). N values for 0.02; 0.03; 0.1 and 0.6% gels (% bis): n=14; 14; 13; 13, respectively. Rheology was performed once to confirm compression testing (solid line). N values for 0.02; 0.1; and 0.6 % gels: n=6, 4, and 4, respectively. . *** $p<0.001$ for compression and $^{xx}p<0.01$ for rheolgy determined by Kruskal-Wallis Test followed by Dunn's Multiple Comparison Test compared to 1 kPa gels.

Effects of stiffness on dendrite branching

We asked whether the stiffness of the substrate on which neurons are grown affects dendritic arborization. Neurons were analyzed at DIV 12 since this is the peak of dendrite branching (17, 79-81). Neurons plated onto gels with a Young's modulus of 8 kPa showed an increase in secondary dendrite number compared to neurons grown on gels of 1 kPa (**Figure 3 A**). Primary dendrite number also showed an increase, but these data were not significant.

In addition, we examined the number of dendrite branches and the total number of dendrites. Neurons grown on gels of 8 kPa contained an increased number of branch points compared to neurons grown on gels of 1 kPa (**Figure 3 B**). Moreover, neurons grown on gels of 2, 8, and 25 kPa all contained a larger number of terminal points compared to neurons grown on gels of 1 kPa (**Figure 3 C**).

To further analyze dendrite branching, we performed Sholl analysis. Sholl analysis is performed by drawing concentric circles at a fixed distance from the cell body. Next, the number of dendrites that intersect each circle is counted. A graph is then generated, showing the number of intersection at specific distances from the cell body (**Figure 4**). This analysis is a method for quantifying the spatial distribution of a dendritic arbor with regards to the cell body. For the purpose of our analysis, we grouped intersections into three categories based on their distance from the cell body: proximal, intermediate, and distal (**Figure 4**). Neurons grown on gels of 8 kPa stiffness showed an increase in the number of proximal and intermediate intersections (15-105 μm from the cell body) compared to neurons grown on 1 kPa gels (**Figure 3 D**). The increase in proximal and intermediate intersections in neurons grown on the 8 kPa gels parallels increases seen in

primary and secondary dendrites seen in **Figure 3 A.**

.

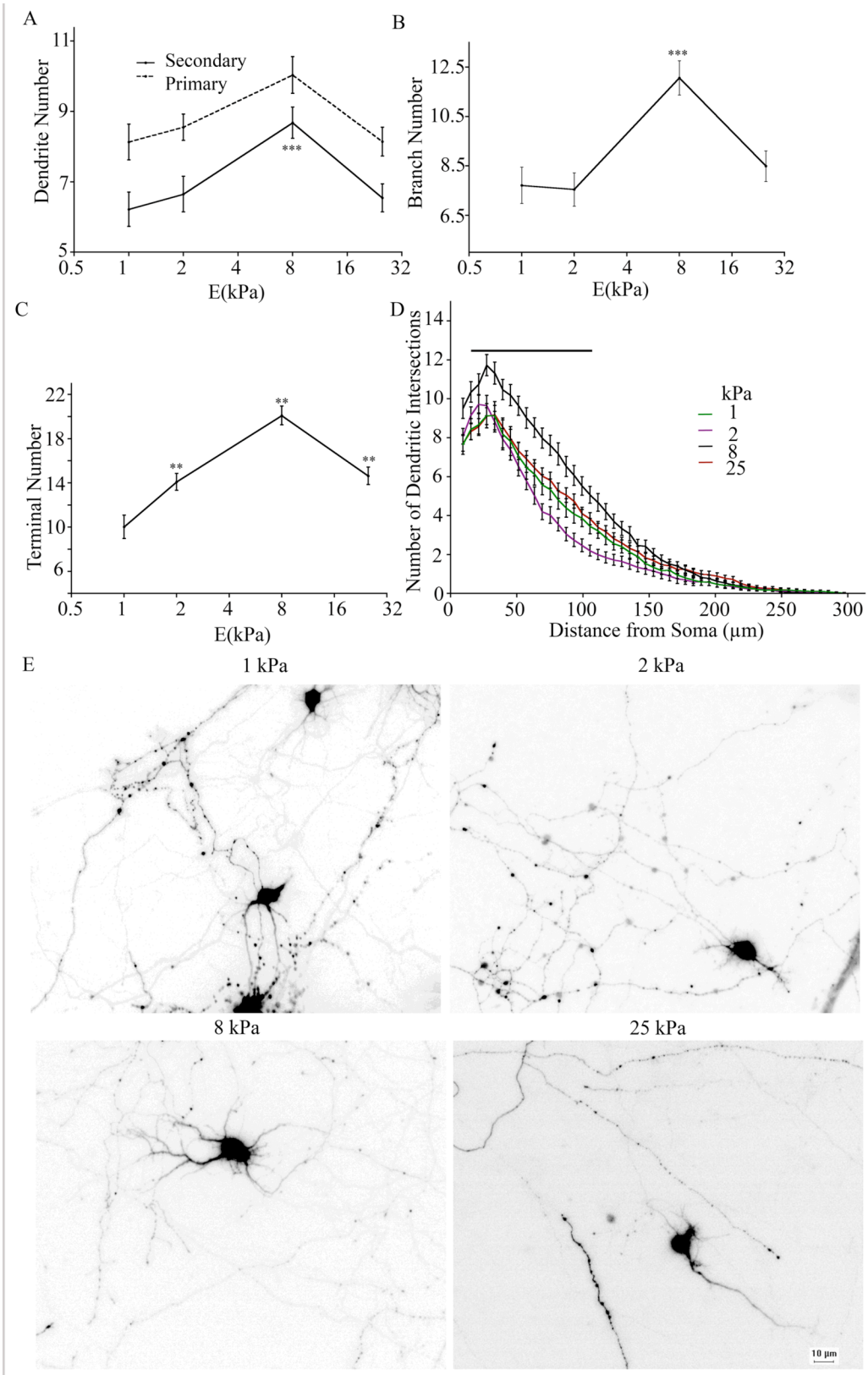

Figure 3. Dendrite number peaks in neurons grown on gels of intermediate stiffness. (A)

Primary dendrite number increases in neurons grown on 8 kPa gels. This increase is marginally significant. Secondary dendrite number peaks in neurons grown on gels of 8 kPa. ***$p<0.001$ for secondary dendrites determined by Kruskal-Wallis Test followed by Dunn's Multiple Comparison Test compared to 1 kPa gels. (B) Branch points increase in neurons grown on 8 kPa gels. ***$p<0.001$ determined by Kruskal-Wallis Test followed by Dunn's Mulitple Comparison Test compared to 1kPa gels. (C) Terminal points increase in neurons grown on 2, 8, and 25kPa gels. **<0.01 determined by ANOVA followed by Dunnett's Multiple Comparison Test compared to 1kPa gels. (D) Sholl analysis. The number of intersections peaks at 15-105 μm (black line) from the soma for neurons grown on 8 kPa gels (see **Appendix Table 3**) (E) Representative images of neurons quantitated in panels A and D. n values are as follows: 1 kPa, n=46; 2 kPa, n=40; 7.5 kPa, n=59; 25 kPa, n=55. Panels A-D show the average values of three experimental trials (mean + SEM). Scale bar, 10 μm.

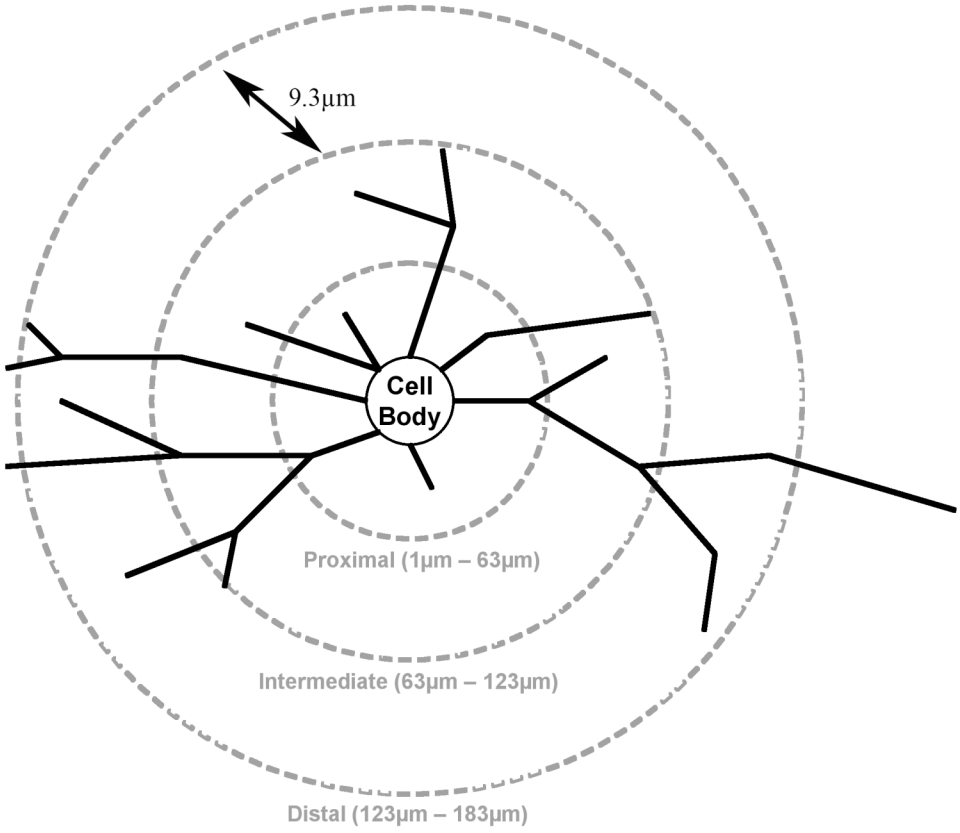

Figure 4: Sholl Analysis. Concentric circles are drawn around the cell body at a fixed distance of 9.3 µm. Number of intersecting dendrites are counted at the fixed distances.

Glutamate receptor regulation

AMPA and NMDA receptors are postsynaptic glutamate-gated receptors that play roles in regulating dendrite branching (82-89). To assess whether these glutamate receptors also play roles in regulating dendrite branching patterns due to changes in extracellular stiffness, neurons were treated with NMDA or AMPA receptor antagonists, APV or CNQX, respectively.

Treatment of neurons with APV

When NMDA receptor activity was blocked with APV, substrate stiffness-dependent changes in the number of primary and secondary dendrites were eliminated (**Figure 5 A**). This was due to an increase in the number of primary and secondary dendrites in neurons grown on 1 kPa, 2 kPa, and 25 kPa gels. Compared to their vehicle-treated controls, however, these increases were only significant for the average number of primary dendrites in neurons grown on 25 kPa gels and the average number of secondary dendrites identified in neurons grown on both 1 kPa and 25 kPa gels.

Moreover, blocking NMDA receptors eliminated substrate stiffness-dependent changes in the number of branch and terminal points. (**Figure 5 B** and **C**). This is again due to the increased number of branch points and terminal points identified in neurons grown on1 kPa, 2 kPa, and 25 kPa gels. These changes were only statistically significant when compared to vehicle-treated controls for the number of branch points in neurons grown on 1 kPa gels, and the number of terminal points in neurons grown on 1 kPa and 25 kPa gels.

Next, we examined the change in branching patterns through the use of Sholl

analysis when neurons on gels were treated with APV. This analysis indicated that when NMDA receptors are blocked, there is no measurable change in the spatial distribution of dendrites on any of the gel rigidities examined (**Figure 5 D**). This analysis was expanded, however, by comparing the Sholl curves for APV-treated cells to the Sholl curves for vehicle-treated conditions for each gel stiffness (**Figure 6**). This additional analysis revealed that APV-treated neurons grown on 1 and 25 kPa gels had an increased number of dendritic intersections (**Figure 6 A** and **D**) compared to the untreated controls. This trend was reversed for the 8 kPa gel, however, on which APV treatment caused a decrease in the number of dendritic intersections (**Figure 6 C**).

Overall, blocking NMDA receptor activity caused an increase in the number of primary dendrites, secondary dendrites, and terminal tips in neurons grown on both 1 kPa and 25 kPa gels and an additional increase in the number of branch points in neurons grown on 1 kPa gels. When NMDA receptors are blocked, increases in these metrics for neurons grown on 8 kPa gels cannot be observed over the elevated baseline. This suggests that NMDA receptors play a role in mediating substrate stiffness-dependent changes in dendritic arborization.

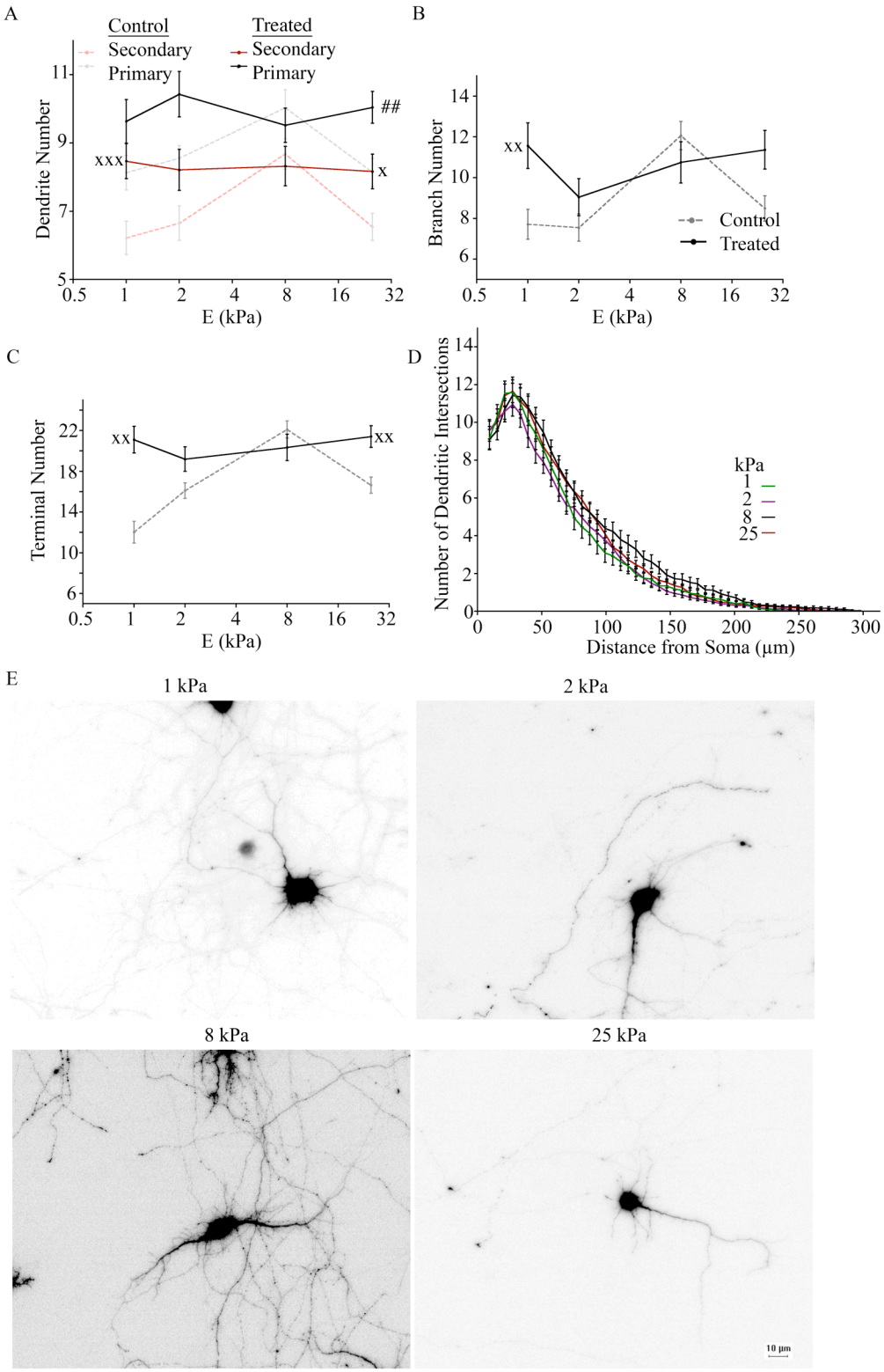

Figure 5. APV treatment eliminates substrate-dependent changes in branching. (A) Primary and secondary dendrite number did not change with APV treatment over the

range of gel stiffnesses examined (solid line). In neurons grown on 1 kPa gels, secondary dendrite number increased with APV treatment (dotted line) compared to vehicle-treated controls. $^{xxx}p<0.001$ determined by Kruskal-Wallis Test followed by Dunn's Multiple Comparison Test. In neurons grown on 25 kPa gels, both primary and secondary dendrite number increased with APV treatment compared to vehicle-treated controls. $^{\#\#}p<0.01$ for primary dendrites determined by Kruskal-Wallis Test followed by Dunn's Multiple Comparison Test and $^{x}p<0.05$ for secondary dendrites determined by ANOVA followed by Dunnett's Multiple Comparison Test. (B) The number of branch points per neuron did not change with increasing stiffness when the neurons were treated with APV (solid line). In neurons grown on 1 kPa gels, the number of branch points increased compared to vehicle-treated control (dotted line). $^{xx}p<0.01$ determined by Kruskal Wallis Test followed by Dunn's Multiple Comparison Test. (C) The number of terminal points per neuron did not change with increasing stiffness when the neurons were treated with APV (solid line). In neurons grown on 1 kPa gels and 25 kPa gels, terminal points increased compared to control (dotted line). $^{xx}p<0.01$ in neurons grown on 1 kPa gels determined by ANOVA followed by Dunnett's Multiple Comparison Test. $^{xx}p<0.01$ in neurons grown on 25 kPa gels determined by Kruskal-Wallis Test followed by Dunn's Multiple Comparison Test. (D) Sholl analysis for neurons treated with APV. There were no significant differences seen in dendrite distribution between different gel stiffnesses. (E) Representative images of neurons quantitated in panels A-D. n values for neurons treated with APV are as follows: 1 kPa, n=30; 2 kPa, n=47; 7.5 kPa, n=56; 25 kPa, n=49. Figure shows a combination of three experiments (mean $\pm$ SEM), which were sister cultures with those shown in Figures 4 and 7. Statistics comparing control with APV treatment were performed with CNQX treatments since the control (vehicle-treated) neurons were shared, and experiments using either antagonist were performed in parallel. Scale bar, 10 μm.

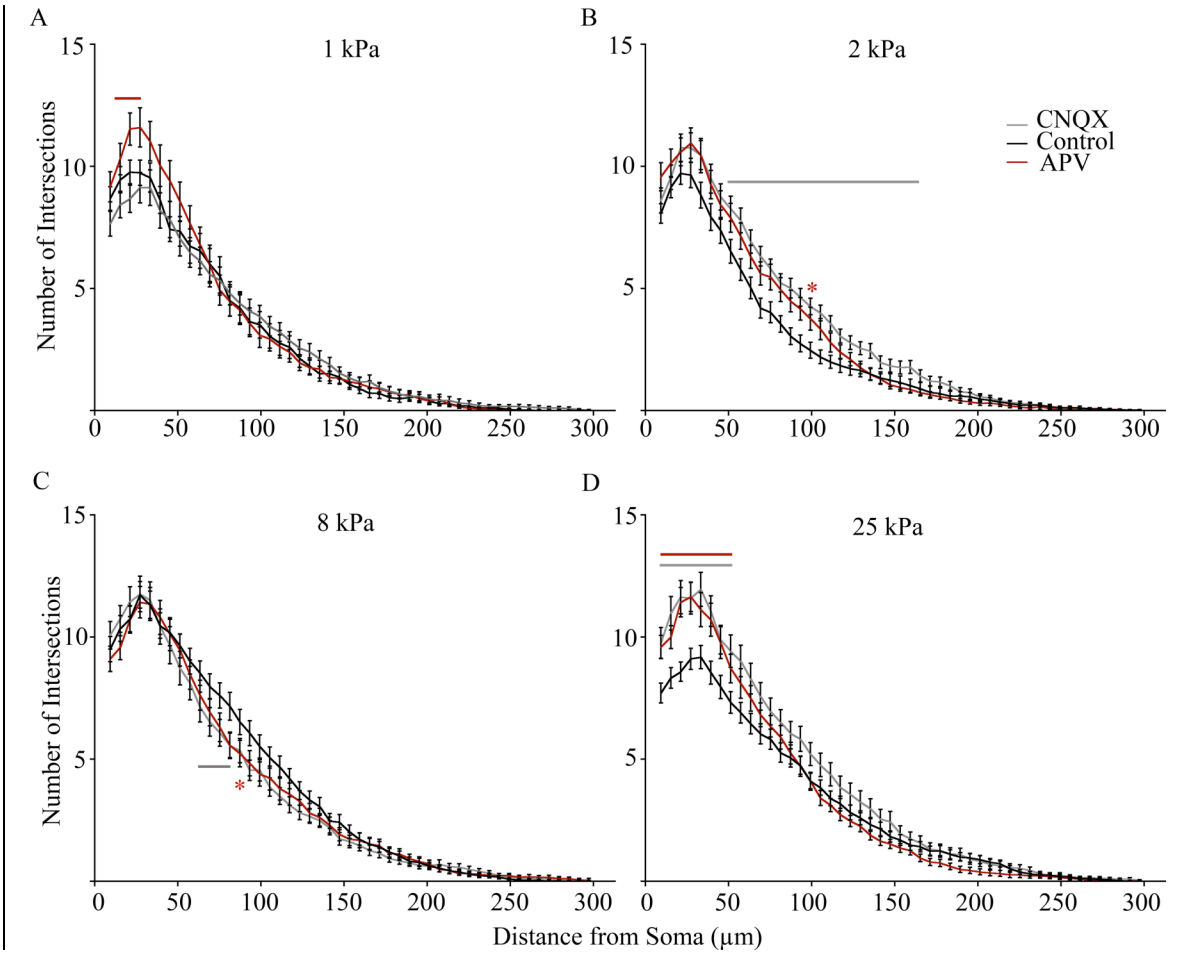

Figure 6. APV and CNQX treatments affect dendrite distribution differently based on distance from the cell body and substrate stiffness. (A) In neurons grown on 1 kPa gels, the number of dendritic intersections within a 15-27 μm radius (red line; proximal region) increased when neurons were treated with APV. (B) In neurons grown on 2 kPa gels, the number of dendritic intersections within a 51-165 μm radius (grey line; the proximal, intermediate, and distal regions) increased when neurons were treated with CNQX, while APV caused an increase at 99 μm (red asterisk; the intermediate region). (C) In neurons grown on 8 kPa gels, however, the number of dendritic intersections decreased within a radius of 75-81 μm (grey line) when neurons were treated with CNQX and at a radius of 87 μm (red asterisk) when neurons were treated with APV (both within the intermediate region). (D) In neurons grown on 25 kPa gels, the number of dendritic intersections occurring within a radius of 9-57 μm (red line) increased due to APV treatment, while CNQX treatment caused an increase within a radius of 9-57 μm (grey bar; both within the proximal region). Figure shows a combination of three experiments. (mean ± SEM; See **Appendix Table 4-7**).

Treatment of neurons with CNQX

Similar to the results observed when NMDA receptor activity was blocked, blocking AMPA receptor activity with CNQX eliminated the substrate stiffness-dependent effects on the number of primary and secondary dendrites (**Figure 7 A**). When compared to vehicle-treated control, only neurons grown on 25 kPa gels had more primary and secondary dendrites in response to CNQX treatment.

Blocking AMPA receptors also increased the number of branch points and terminal points on 25 kPa gels (**Figure 7 B** and **C**). Compared to vehicle-treated controls, the number of terminal points in neurons grown on 1 kPa gels and 25 kPa increased and the number of branch points in neurons grown on 25 kPa increased with CNQX treatment (**Figure 7 B** and **C**).

Sholl analysis of CNQX-treated neurons showed that neurons grown on 25 kPa gels had an increase in the number of dendrite intersections found in proximal, intermediate, and distal fields when compared to neurons grown on 1kPa gels (**Figure 7 D**). Sholl analysis of CNQX-treated neurons showed that neurons grown on 8 kPa gels had an increase in the number of distal dendrites when compared to neurons grown on 1 kPa gels (**Figure 7 D**). As a follow up, we again examined the affects of CNQX treatment compared to vehicle-treated controls for each stiffness (**Figure 6**). In neurons grown on 2 kPa and 25 kPa gels, CNQX treatment increased the number of dendritic intersections compared to vehicle-treated controls (**Figure 6 B and D**). In neurons grown on 8 kPa gels, however, this change was reversed and the number of dendritic intersections decreased in response to CNQX treatment (**Figure 6 C**).

Overall, blocking AMPA receptor activity caused an increase in the number of

terminal points and branch points in neurons grown on 25 kPa gels and an increase in the number of terminal points in neurons grown on 1 kPa gels. When AMPA receptors were blocked, increases in these metrics for neurons grown on 8 kPa gels could not be observed over the elevated baseline. This suggests that AMPA receptors play a role in mediating substrate stiffness-dependent changes in dendritic arborization.

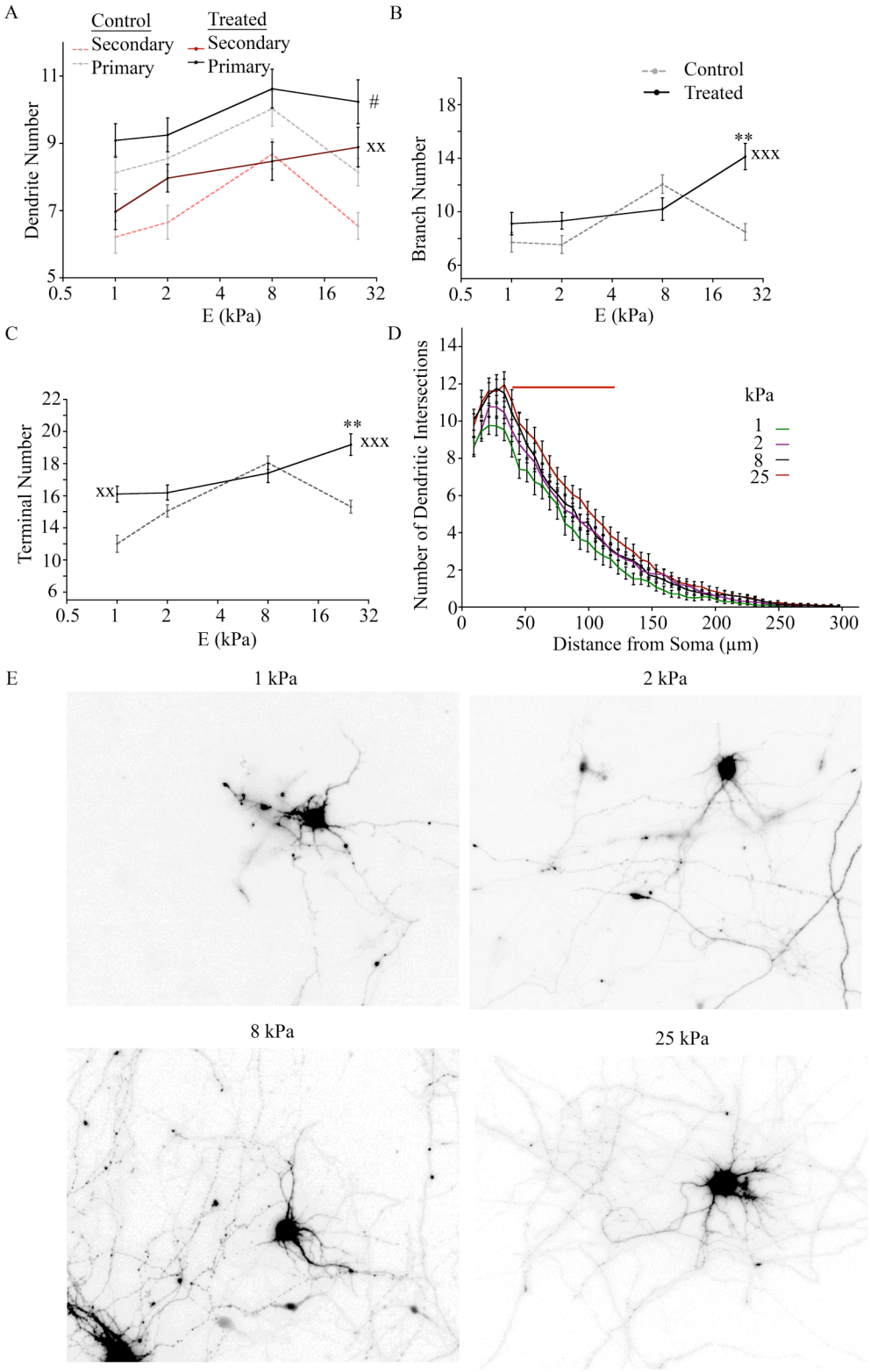

Figure 7. CNQX treatment increases dendrite branching in neurons grown on 25 kPa gels. (A) Primary and secondary dendrite number did not change with CNQX

treatment,over the range of gel stiffnesses examined (solid line). In neurons grown on 25 kPa gels, secondary dendrite number increased with CNQX treatment relative to vehicle-treated controls. $^{\#}p<0.05$ and $^{xx}p<0.01$ determined by Kruskal-Wallis Test followed by Dunn's Multiple Comparison Test, (B) The number of branch points increased in neurons grown on gels of increasing stiffness when the neurons were treated with CNQX (solid line). **p<0.01 determined by Kruskal-Wallis Test followed by Dunn's Multiple Comparison Test. In neurons grown on 25 kPa gels, the number of branch points increased compared to control (dotted line). $^{xxx}p<0.001$ Kruskal-Wallis Test followed by Dunn's Multiple Comparison Test. (C) The number of terminal points increased in neurons grown on gels of increasing stiffness when the neurons were treated with CNQX (solid line). **p<0.01 determined by Kruskal-Wallis Test followed by Dunn's Multiple Comparison Test. In neurons grown on 1 kPa gels, terminal points increased compared to control. $^{xx}p<0.01$ determined by ANOVA followed by Dunnett's Multiple Comparison Test. In neurons grown on 25 kPa gels, the number of branch points increased compared to control (dotted line). $^{xxx}p<0.001$ Kruskal-Wallis Test followed by Dunn's Multiple Comparison Test. (D) Sholl analysis for neurons treated with CNQX. The number of dendritic intersections within a radius of 45-135 μm (red line) and 135 μm (black asterisk) from the cell body was increased in neurons grown on 25 kPa and 8 kPa gels, respectively, with CNQX treatment (see **Appendix Table 8**). (E) Representative images of neurons quantitated in panels A-D. n values for neurons treated with CNQX: 1 kPa, n=35; 2 kPa, n=56; 7.5 kPa, n=51; 25 kPa, n=47. Figure shows a combination of three experiments, which were sister cultures with Figures 5 and 6 (mean $\pm$ SEM). Statistics comparing control with APV treatment were performed with CNQX treatments since the control (vehicle-treated) neurons were shared, and experiments using either antagonist were performed in parallel. Scale bar, 10 μm.

AMPA and NMDA receptors modulate spatial distribution of dendrites

The studies above suggest that both AMPA and NMDA receptors play a role in mediating the neuronal response to mechanical properties of the substrate on which the neurons are grown. Because changes in branching behavior do not necessarily affect all regions of the dendritic arbor equally, we assessed whether the role of NMDA and AMPA receptors in regulating dendrite branching is global or local to specific sub-regions of the arbor.

Blocking NMDA receptor activity caused a change in dendrite number proximal and/or intermediate to the cell body across all stiffness ranges. Sholl analysis shows that APV treatment increased the number of proximal dendritic intersections (15-27 μm) for neurons grown on 1 kPa gels (**Figure 6 A**). Similarly, blocking NMDA receptor activity increased the number of dendritic intersections in the intermediate region (at 99 μm) for neurons grown on 2 kPa gels (**Figure 6 B**). These increases were not observed on the 8 kPa gels, where APV treatment reduced the number of dendritic intersections in the intermediate range (at 81 μm; **Figure 6 C**). However, APV treatment increased the number of proximal dendritic intersections (9-57 μm) for neurons grown on the stiffer substrates (25 kPa) (**Figure 6 D**).

AMPA receptors appear to regulate dendrite distribution in a way that is dependent on the stiffness of the neuronal growth substrate. For example, Sholl analysis shows that CNQX treatment has no effect on the number of dendritic intersections for neurons grown on 1 kPa gels (**Figure 6 A**). CNQX treatment increased the number of intermediate and distal dendritic intersections for neurons grown on 2 kPa gels (51-165 μm; **Figure 6 B**). Furthermore, CNQX treatment increased the number of proximal

dendritic intersections (9-57 μm) for neurons grown on 25 kPa gels (**Figure 6 D**). On the 8 kPa gels, however, the number of dendritic intersections was largely unchanged by AMPA receptor blockade, except in the intermediate range, from 63-75 μm, where the number of intersections decreased compared to vehicle-treated controls (**Figure 6 C**).

Both NMDA receptors and AMPA receptors appear to play a role in modulating substrate stiffness-dependent changes in dendritic distribution (**Table 1**). However, Sholl analysis suggests that their effects are most prominent in different regions of the dendritic arbor.

Dendrite Branchingin Neurons Plated on Glass

Next, we wanted to observe if dendrite branching differs when glass is used as a substrate, which is the traditional way of plating neurons, compared to plating on soft substrates. Neurons were plated on glass at the same density as on gels (**Figure 8**). The number of primary and secondary dendrites, as well as the number of terminal points increased for neurons grown on 8 kPa gels compared to neurons grown on glass. Moreover, neurons grown on 1 kPa gels showed a decrease in the number of branch and terminal points compared to neurons grown on glass (**Figure 8 B**). 1 kPa gels are similar to the stiffness of the rat brains (52). Thus, dendrite branching seen in neurons grown on substrates with similar stiffness to that of the brain is different than that seen in neurons plated on glass.

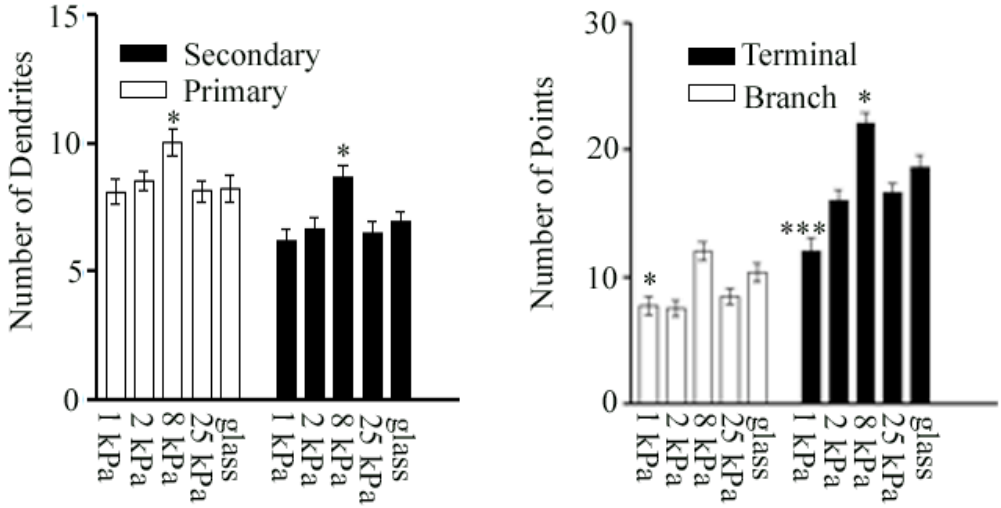

Figure 8: Dendrite branching in neurons plated on glass is different then that seen in neurons plated on hydrogels. (A) Primary and secondary dendrite number increased for neurons grown on 8 kPa gels compared to neurons grown on glass *$p<0.05$ determined by Krutsal Wallis followed by Dunn's Multiple Comparison Test (B) Branch point and terminal number decreased for neurons grown on 1 kPa gels compared to neurons grown on glass. Terminal point number increased for neurons grown on 8 kPa gels compared to neurons grown on glass. *$p<0.05$ and ***$p<0.001$ determined by Krutsal Wallis followed by Dunn's Multiple Comparison Test.

DISCUSSION

Plating neurons on glass is the traditional method used for studying dendrite branching (1, 18, 28). This is not the most physiological way to study dendrite development because glass is stiffer than the brain. Our studies show that neurons plated on glass show different dendrite branching parameters compared to neurons plated on various gel rigidities.

Previous studies of neuronal growth on hydrogels have shown that neurite number increases with increasing gel stiffness (31, 33). Our data show that over the range of 1 kPa to 25 kPa, branching reaches a maximum in neurons grown on gels of an intermediate stiffness, 8 kPa in our experimental system.

Our studies also aim to identify a mechanism by which neuron sense extracellular stiffness to regulate their dendritic arbors. Based on previous observations that glutamate receptors can regulate dendrite branching in a variety of neurons (82-89), we used receptor antagonists as a means of probing the role of NMDA and AMPA receptors in generating these substrate-dependent morphological characteristics. Our data show that NMDA and AMPA receptors play different roles in regulating dendrite branching patterns in neurons grown on gels of different compliances. We find that NMDA receptors play a role in regulating characteristics of the dendritic arbor close to the cell body, while AMPA receptors play a role in determining arbor characteristics over a broader spatial range but only in cells grown on substrates with stiffnesses above a certain threshold (2 kPa; **Figure 9** and **Table 1**).

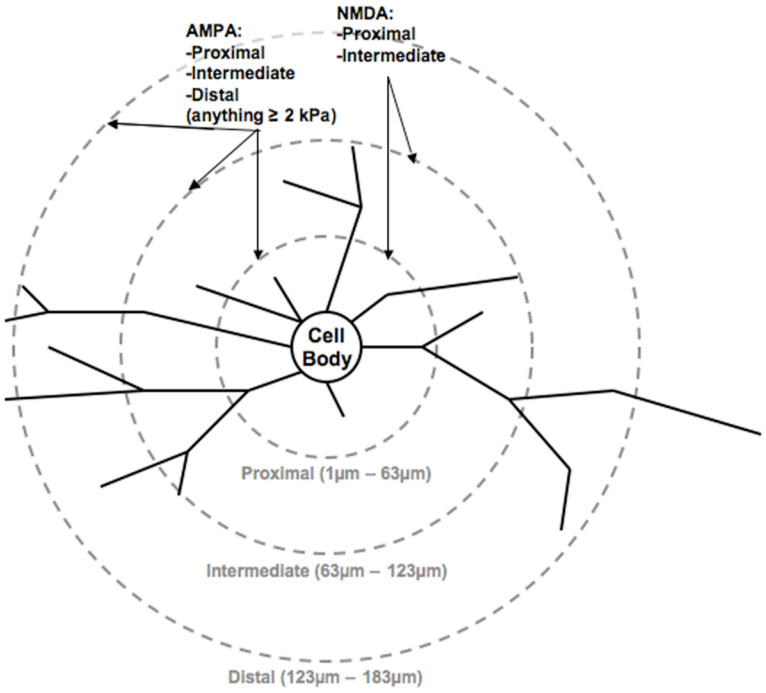

Figure 9. Model of action of NMDA and AMPA receptors on dendrite morphology. AMPA receptors play a role in dendritc arborization for harder stiffness, ≥2kPa, at all distances from the cell body. NMDA receptors play a role in dendritic arborization for a range of rigidities (1-25 kPa), only proximal and intermediate lengths from the cell body.

Treatment	APV					CNQX			
Stiffness (kPa)	1	2	8	25		1	2	8	25
Primary Dendrite Number				↑					↑
Secondary Dendrite Number	↑			↑					↑
Branch Points	↑								↑
Terminal Points	↑			↑		↑			↑
Proximal Arborization	↑			↑			↑	↓	↑
Intermediate Arborization		↑	↓				↑	↓	
Distal Arborization							↑		

Table 1. Summary table on effects of NMDA and AMPA antagonists on dendrites. Boxes are marked when treatment above affected parameter listed on left. Arrows indicate significant trend compared to vehicle-treated control.

Over the range of substrate rigidities examined by other groups, neurons adhere to and branch more on harder substrates than on softer substrates (31). We have discovered, however, that under certain conditions, there is an optimal stiffness that enhances dendrite branching that does not simply maximize the stiffness of the growth substrate. . Our data conflict with some previous reports that observe that as substrate stiffness increases, dendrite branching decreases (53, 90). This discrepancy could be due to many reasons: cell type, cell density, substrate stiffness range, analysis methods, culture density, and cell age *in vivo* and *in vitro* (33).

The mechanism by which substrate stiffness regulates cellular morphology is most likely analogous to the mechanisms controlling other cellular activities, such as cell motility, that are dependent on cytoskeletal remodeling. Cell migration is highly dependent on the adhesiveness of the cell to the substrate (91). There is an optimal adhesion force, below which the cells slip at the leading edge and above which they fail to release at the trailing edge (92). Either of these processes inhibits forward motion of the cell, meaning that an intermediate adhesive force to the substrate maximizes migration speed (91). This same concept may apply to dendrite morphology since adhesion affects dendrite branching (93); if the substrate is too hard, the adhesion forces will hinder the ability of the dendrite to branch.

Activation of AMPA receptors attenuates dendrite growth, and inhibition of NMDA receptor activity increases branching (94, 95). Other studies conflict with results from previous studies and this study in that they show that inhibition of NMDA and AMPA receptor activity decreases dendrite branching (29, 87). In our experiments, we blocked these glutamate receptors to determine the roles they play in regulating substrate

stiffness-induced changes in dendrite morphology. Our studies show that AMPA receptors play a role in determining dendrite patterning throughout the entire length of the dendritic arbor, whereas NMDA receptors play a role in determining dendrite patterning only proximal to the soma. This variation in regulation of dendrite morphology by glutamate receptors may be due to receptor distribution (96-99). Our study moves one step further, showing that these separate effects of NMDA or AMPA receptor blockade are dependent on substrate rigidities. Traditional theory suggests that we would expect to see an increase in branching when neurons were treated with an NMDA or AMPA receptor antagonist. However, blocking these receptors only resulted in a significant increase in branching parameters on 1 kPa and 25 kPa gels for NMDA receptor-inactivated neurons and on 25 kPa gels for AMPA receptor-inactivated neurons.

There are multiple factors that may play roles in determining changes in neuronal morphology occurring on substrates with different mechanical properties. Determining the role of glutamate receptors in regulating dendrite arborization adds another level of complexity. The final arbor is likely to be the product of the sensitization of the neuron to different activation cues. For example, differences in glutamate receptor blockade may be due to the distinct spatial distribution of the receptor types, and thus, the substrate stiffness-dependent observations we make may be caused by a change in the relative membrane concentrations of AMPA and NMDA receptors (96, 98-100). A reason for the differences in the roles NMDA and AMPA receptors play may be due to integrin activation. Integrins are heterodimer adhesion molecules that are involved in cell-cell and cell-extracellular matrix interactions. Both NMDA and AMPA receptors are influenced by the stimulation of integrins (101-103), which show an increase in expression in

neurons grown on stiffer substrates (51). Previous work has shown that NMDA receptors activate with high and low stimulation of integrins by high and low concentrations of RGD, respectively (104). AMPA receptor activity increases with high integrin stimulation, whereas AMPA receptor activity decreases with low integrin stimulation (104). This window between high and low integrin activation, where NMDA and AMPA receptors behave differently, provides a potential explanation for how increasing substrate stiffness may create a differential effect based on selective inactivation of either NMDA or AMPA receptors. One interpretation consistent with our studies is that on soft gels, integrin activation is lower than on harder gels, so AMPA receptors are not active and will not play a role in shaping the dendritic arbor. By comparison, on hard gels, AMPA receptors are active and play an important role in determining dendrite distribution. To test this theory, future studies will address the role of integrins and other signaling systems in shaping the dendritic arbors of hippocampal neurons grown on substrates of different rigidities.

CHAPTER 1b: Substrate stiffness affects the dendrite patterning of hippocampal neurons independent of cell density.

INTRODUCTION

A century ago, Ramon y Cajal determined that thorough examination of neuronal dendrite morphology would help to elucidate overall nervous system function. Dendrite branching is a highly dynamic process and determines the role a neuron will play in a neuronal circuit (105-107). Proper development of the dendritic arbor is important for normal nervous system function; abnormalities in dendrite branching patterns occur in a number of cognitive disorders, including Alzheimer's disease, Down syndrome, autism, Rett syndrome, and schizophrenia (15, 108, 109).

The development of the dendritic arbor is a multi-stage process and is influenced by numerous intrinsic and extrinsic factors (17, 110). Recently, it has been shown by a number of groups, including our own, that the molecular mechanisms underlying the trafficking of receptors and signaling elements to postsynaptic sites also help to shape the dendritic arbor (29, 111). In the current study, we examined the effects of substrate stiffness on the dendrite morphology when hippocampal neurons were grown on compliant substrates. We also examined the effects of cell density on dendrite branching parameters.

In our studies and in previously published work, increased substrate stiffness results in an increase in cell density due to differences in cell adhesion (30-32). Furthermore, cell density affects dendrite morphology due to variation in cell-cell contact, synaptic density, and global concentration of extrinsic factors (17, 79, 112-115). Thus, it is of importance to examine whether cell density in mixed neuronal cultures plays a role in determining the dendrite branching phenotypes seen in neurons grown on hydrogels of varying rigidities.

In this study, we grew mixed cultures of hippocampal cells on polyacrylamide (PA) gels to assess the effects of varying cell densities on two different substrate rigidities. PA gels are used in this study because we are able to make substrates with varying rigidities by varying the percentage of the crosslinker, bis-acrylamide (30, 51, 116). In addition, varying the percentage of crosslinker does not vary the pore size or amount of adhesion sites on the gels (30, 51, 52, 116). We observed that substrate stiffness plays a larger role in determining branching patterns than does cell density. However, cell density does indeed influence dendrite branching.

MATERIALS AND METHODS

Antibodies

Neurons were immunostained using anti-MAP2 (Chemicon, Temecula, CA), mature astocytes were immunostained using anti-GFAP (Chemicon, Temecula, CA), and immature astrocytes were immunostained using anti-vimentin (Chemicon, Temecula, CA). Microglia were immunostained using anti-OX42 and oligodendrocytes were immunostained using anti-CNPase (Chemicon, Temecula, CA).

PA Gel Preparation, Primary Neuronal Culture, Transfection Dendrite Analysis and Imaging, and Statistics

See Chaper 1a.

Immunocytochemistry

Cultures were fixed at the indicated time points. Neurons were blocked and permeabilized in blocking solution containing 5% normal goat serum and 0.1% Triton X-100 in PBS. Neurons were immunostained using a 1:500 dilution of the indicated antibody for 1-2 hours at room temperature or overnight at 4°C and then for 1-2 hours with a secondary antibody conjugated to fluorophore (Jackson ImmunoResearch, West Grove PA).

RESULTS

Cell density increases with increasing stiffness and initial plating density

We first determined the adhesion and densities of specific cell types on various gel rigidities. We plated mixed cultures of hippocampal cells on gels ranging from 0.02 to 0.6% bis-acrylamide at an initial plating density of 60,000 cells/cm^2. Previously published work has shown that as the percentage of bis-acrylamide increases, the stiffness of the gel increases (32, 51). Cultures were fixed on 12 DIV and immunostained with various cell markers. We observed that as percent bis-acylamide increased, the density of neurons (MAP2-positive cells) and mature astrocytes (GFAP-positive cells) increased (**Figure 10**). The number of immature astrocytes (vimentin-positive cells) did not change as percent bis-acrylamide increased (**Figure 10**). We also immunostained the cultures to determine the number of microglia and oligodendrocytes present. However, very few, if any, of these cell types were present (data not shown).

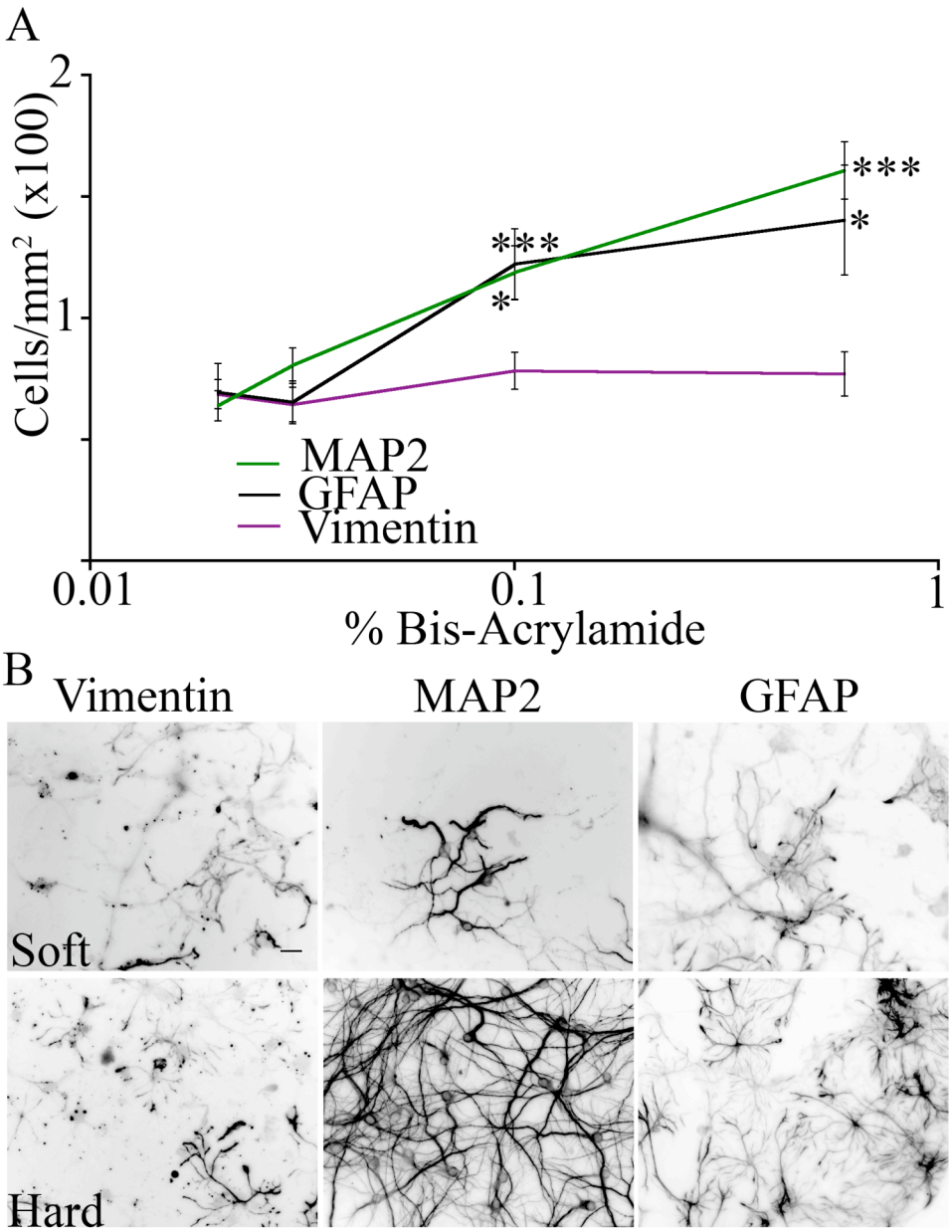

Figure 10. As percent bis-acrylamide increases in the polyacrylamide gel, the number of neurons and astrocytes increases as assessed on 12 DIV. (A) The number of neurons and mature astrocytes increases as gel stiffness increases. The number of immature astrocytes does not change when the cells are plated on gels of different densities. ***$p<0.001$ for MAP2-positive cells and *$p<0.05$ for GFAP-positive cells determined by Krustal-Wallis Test followed by Dunn's Multiple Comparison Test compared to 0.02% bis-acrylamide gels. (B) Representative images quantitated in A. The data shown are from three experiments. Numbers of pictures taken for each condition are listed for 0.02, 0.03, 0.1, and 0.6% bis-acrylamide gels, respectively. Vimentin: n=43; 34; 44; 31. MAP2: n=35; 34; 30; 35. GFAP: n=29; 39; 38; 29. Scale bar, 10 μm.

When gels, with the same initial plating densities, were compared on 12 DIV, cells did not always adhere to or grow better on hard gels than soft gels. When grown on hard gels, more neurons and astrocytes were present when plated at an initial density of 50,000 cells/cm^2 (**Figure 11 A, D, F** and **G**). However, when cells were plated at an initial density of 80,000 cells/cm^2, only mature astrocytes showed an increased number when grown on hard versus soft gels (**Figure 11 B, D, F** and **G**). Moreover, when cells were plated at an initial density of 100,000 cells/cm^2, more neurons, but not astrocytes, adhered to and grew on hard gels (**Figure 11 C, D, F** and **G**). These data demonstrate that there is a maximum threshold for the number of astrocytes that will adhere to and grow on hard gels. On soft gels, the numbers of adhering neurons and astrocytes increased when plated at increasing initial densities.

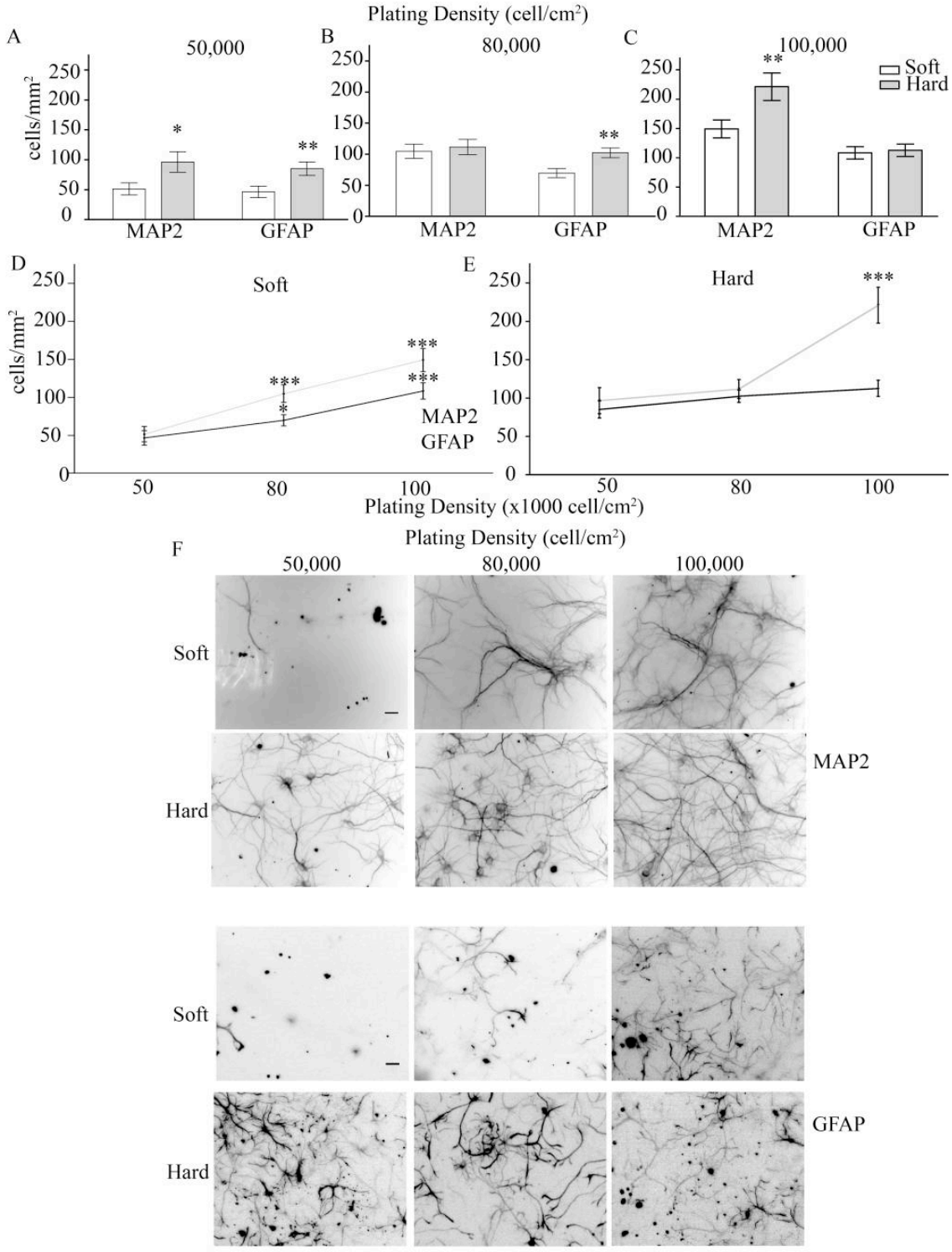

Figure 11. Cell density changes with substrate stiffness and initial plating density as assessed on 12 DIV. (A) The number of neurons and mature astrocytes increases when the cells are plated on hard gels compared to those plated on soft gels with initial density

of 50,000 cells/cm^2. *p<0.05 for MAP2-positive cells and **p<0.01 for GFAP-positive cells determined by Mann Whitney Test. (B) Only the number of mature astrocytes increases when cells are grown on hard gels compared to those grown on soft gels with initial plating density of 80,000 cells/cm^2. **p<0.01 determined by Mann Whitney Test. (C) Only the number of neurons increases when cells are grown on hard gels compared to those grown on soft gels when plated at an initial density of 100,000 cells/cm^2. **p<0.01 determined by Mann Whitney Test. (D) When grown on soft gels, the number of neurons and mature astocytes increases as initial plating density increases. *p<0.05 for GFAP-positive cells and ***p<0.001 for MAP2-positive and GFAP-positive cells determined by Krustal Wallis Test followed by Dunn's Multiple Comparison Test compared to 50 cells/cm^2. (E) As initial plating density increases, the number of neurons increases and the number of mature astrocytes remains unchanged on hard gels. ***p<0.001 for MAP2-positive cells determined by Krustal Wallis Test followed by Dunn's Multiple Comparison Test compared to 50,000 cells/cm^2. (F) and (G) Representative images of MAP2- and GFAP-positive cells, respectively, quantitated in A-E. The data shown are from four experiments. Numbers of picture taken for each condition are listed from 50,000, 80,000, and 100,000 cells/cm^2, respectively. GFAP, soft gels: n=30; 35; 35, and hard gels: n=25; 30; 30. MAP2, soft gels: n= 34; 36; 35, and hard gels: n=25; 36; 30. Scale bar, 10 μm.

We then asked whether the differences in cell number, discussed above, are due to differences in cell adhesion during plating. Cells were plated onto gels at 60,000 cells/cm^2. Neurons were fixed at 24 and 48 hours after plating and immunostained for MAP2. We also immunostained for GFAP, but we found that these time points are too early in culture to observe mature astrocytes. At both 24 and 48 hours after plating, we observed the same trend in the number of neurons found on the gels as we observed on 12 DIV. We found that as the percentage of bis-acrylamide increased, the number of neurons found on the gels increased (**Figure 12**). Thus, the increase in the number of neurons seen on harder gels may be due, at least in part, to increased cell adhesion on stiffer substrates during the initial plating.

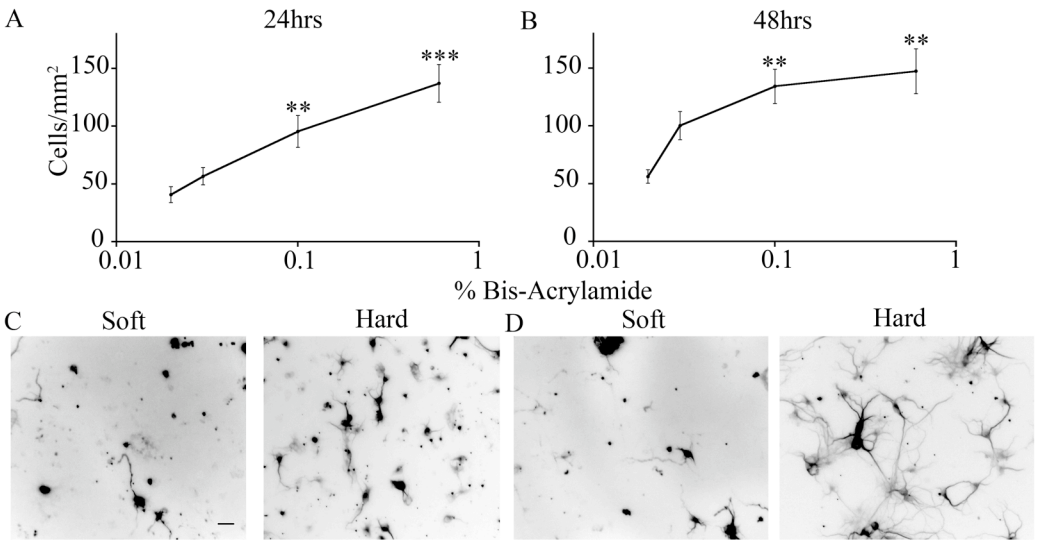

Figure 12. Differences in cell number occur early in culture. Cells were plated at initial densities of 60,000 cells/cm^2. (A) Number of neurons was determined 24 hours after plating. **p<0.01 and ***p<0.001 determined by Krustal Wallis Test followed by Dunn's Multiple Comparison Test compared to cultures grown on 0.02% bis-acrylamide gels. (B) Number of neurons was determined 48 hours after plating. **p<0.01 determined by Krustal Wallis Test followed by Dunn's Multiple Comparison Test compared to cultures grown on 0.02% gels. (C) and (D) Representative images of neurons quantitated on 0.02 and 0.06 % bis-acrylamide gels in figures A and B, respectively. Numbers of pictures taken for each condition are listed for cultures grown on 0.02, 0.03, 0,01, and 0.06% bis-acrylamide gels, respectively. 24 hours: n=30; 55; 56; 55. 48 hours: n=43; 49; 54; 55. Scale bar, 10 μm.

Cell density affects dendrite branching

Since cell density affects dendrite morphology (17, 79, 112-115), we assessed dendrite morphology in neurons grown on our gels. Cells were plated at initial densities of 50, 80, and 100 cells/cm^2 on either hard or soft gels and were fixed on 12 DIV. At equivalent initial plating densities, neurons grown on hard gels consistently have more primary and secondary dendrites than neurons grown on soft gels (**Figure 13 A-C** and **F**). The number of primary and secondary dendrites in neurons grown on soft gels does not change as plating density is increased (**Figure 13 D** and **F**). In contrast, neurons grown on hard gels show a decrease in primary and secondary dendrite numbers as plating density increased (**Figure 13 E**). Thus, cell density affects dendrite branching patterns when neurons are grown on hard gels but not soft gels.

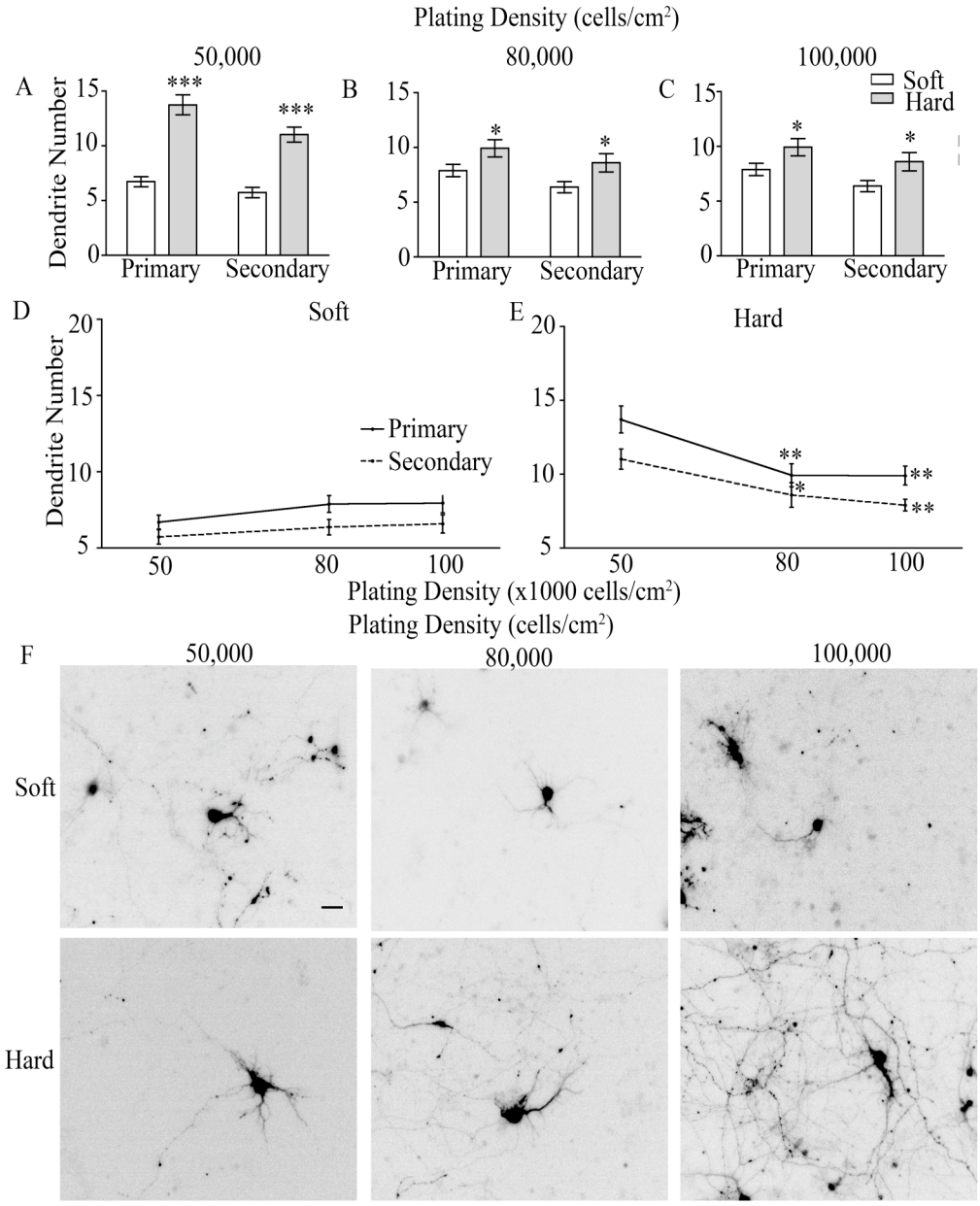

Figure 13. Branching patterns change in neurons grown at different initial plating densities and on different substrate rigidities as assessed on 12 DIV. (A-C) Neurons grown on hard gels have more primary and secondary dendrites than those grown on soft gels with the same initial plating density. ***$p<0.0001$ and *$p<0.05$ determined by Mann Whitney Test. (D) The number of dendrites is independent of initial plating density for neurons grown on soft gels. (E) Neurons grown on hard gels have less primary and secondary dendrites when plated at higher initial cell densities. **$p<0.01$ for primary dendrite number determined by ANOVA followed by Dunnett's Multiple Comparison Test compared to initial plating density of 50,000 cells/cm^2. *$p<0.05$ and **$p<0.01$ for secondary dendrites determined by Krustal-Wallis Test followed by Dunn's Multiple Comparison Test compared to initial plating density of 50,000 cells/cm^2. (F)

Representative images quantitated in A-E. Data are from four experiments. Numbers of cells for each condition are listed for 50,000, 80,000, and 100,000 cells/cm^2, respectively. Soft gels: n= 30; 37; 34. Hard gels: 35; 30; 34. Scale bar, 10 μm.

To fully understand how stiffness and cell density affect dendritogenesis, we examined additional branching parameters, including the number of branch points and total dendrite number. We measured the total number of dendrites by counting the number of terminal points. As expected, dendrites of neurons grown on the harder gels had more terminal points than those of neurons grown on the soft gels at all plating densities (**Figure 14 A-C**). In addition, the number of terminal points decreased as plating density increased for neurons grown on hard gels only (**Figure 14 D** and **E**). These data coincide with the data for primary and secondary dendrite number. Thus, as density increases, dendrite number decreases in neurons grown on hard gels. However, neurons grown on hard gels always have more dendrites than those neurons grown on soft gels at all plating densities.

Similar to terminal point number, dendrites of neurons grown on hard gels have more branch points than dendrites of neurons grown on soft gels at all plating densities (**Figure 14 A-C**). The number of branch points did not change with increases in initial plating density for dendrites of neurons grown on soft or hard gels (**Figure 14 D** and **E**). These data show that the number of branch points found in dendrites of neurons grown on gels of both rigidities is not affected by initial plating density.

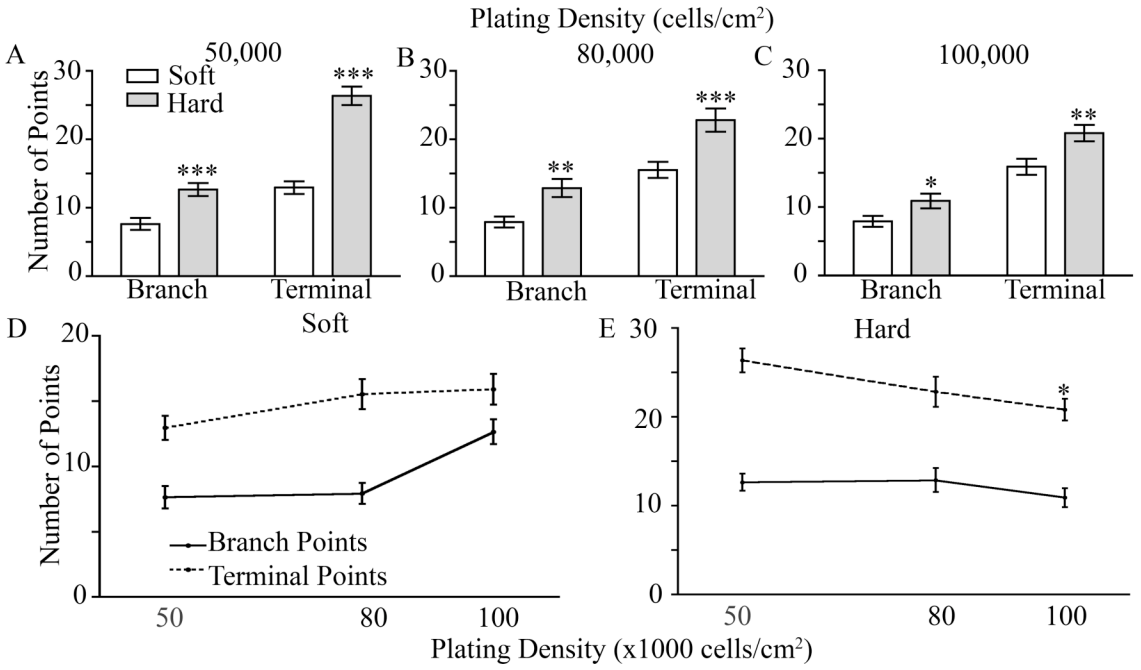

Figure 14. Initial plating density and gel stiffness affect dendrite patterning as assessed on 12 DIV. (A) Numbers of dendrite branch points and terminal points increase in neurons grown on hard gels compared to those grown on soft gels when plated at an initial density of 50,000 cells/cm^2. ***p<0.0001 determined by Mann Whitney Test. (B) Numbers of dendrite branch points and terminal points increase in neurons grown on hard gels compared to those grown on soft gels when plated at an initial density of 80,000 cells/cm^2. **p<0.01 for branching determined by Mann Whitney Test and ***p<0.0001 for terminal points determined by Student's t Test. (C) Number of dendrite branch points and terminal points increase in neurons grown on hard gels compared to those grown on soft gels when plated at an initial density of 100,000 cells/cm^2. *p<0.05 for branching points determined by Student's t Test, Welch corrected. **p<0.01 for terminal points determined by Student's t Test. (D) Number of dendrite branch points and terminal numbers do not change in neurons grown on soft gels at different initial plating densities. (E) Number of dendrite branch points does not change, but number of terminal points decreases in neurons grown at increasing plating densities on hard gels. *p<0.05 determined by ANOVA followed by Dunnett's Multiple Comparison Test compared to 50,000 cells/cm^2. Data are from four experiments.

To confirm that dendrite branching patterns differ when initial plating densities differ, we performed Sholl analysis on the neurons. Sholl curves from analysis of dendrites of neurons grown on soft gels were the same, regardless of the initial plating density (**Figure 15 A**). However, there was a decrease in proximal dendrite intersections in dendrites of neurons grown on hard gels when initial plating densities were increased (**Figure 15 B**). These data suggest that cell density plays a role in shaping the dendritic arbor close to the cell body.

We then assessed the role of substrate stiffness on overall dendrite branching patterns. Proximal and intermediate dendritic intersections were higher when neurons were plated on hard versus soft gels for all initial plating densities (**Figure 16**). These data coincide with those indicating changes in primary and secondary dendrite number and terminal branch point number. Together, these data show that the role of substrate rigidity is independent of cell density in shaping the dendritic arbor.

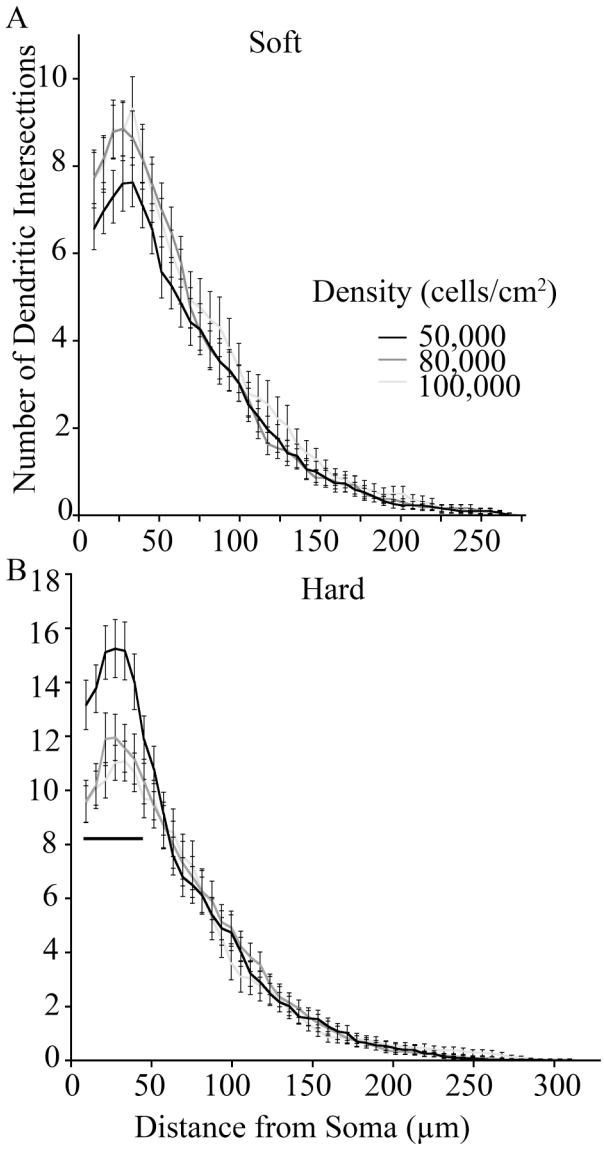

Figure 15. Sholl analysis of neurons grown at different initial plating densities. (A) Initial plating density has no effect on dendrites when neurons are grown on soft gels. (B) When plated at the lowest density (50,000 cells/cm^2), neurons grown on hard gels have the most proximal dendrites (**Appendix Table 9**). Data are from four experiments.

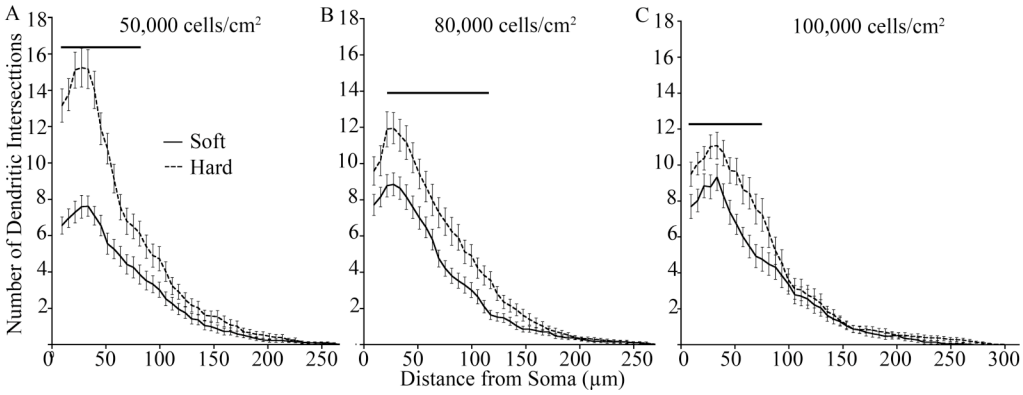

Figure 16. Sholl analysis of neurons grown on gels of varying rigidities. (A) Sholl analysis of neurons grown at an initial plating density of 50,000 cells/cm^2 (B) Sholl analysis of neurons grown at an initial plating density of 80,000 cells/cm^2 (C) Sholl analysis of neurons grown at an initial plating density of 100,000 cells/cm^2. For all conditions, neurons have increased proximal and intermediate branches when grown on hard versus soft gels. (**Appendix Tables 10-12**, respectively). Data are from four experiments.

DISCUSSION

Although there are reports that substrate stiffness plays a role in determining how dendrites branch, as of yet, there are limited studies addressing whether these effects are due to differential adhesion and growth of neurons and/or glia on gels of differing rigidities. Numerous studies have shown that neuronal and glial interactions influence branching (117-119). Specifically, one study by Jiang *et al.* has shown that the interaction between neurons and glia plays a significant role in determining dendrite branching patterns in neurons grown on hydrogels (32). In addition, several studies by our group and others have shown that the number of neurons and glia also change with stiffness (30-32). Thus, neuron-glia interactions may play a role in mediating changes in dendrite branching of neurons grown on hydrogels.

In the current study, we used mixed cultures of hippocampal cells grown on polyacrylamide gels to address whether differences in dendrite branching due to changes in substrate stiffness are independent of cell density. We observed that as substrate stiffness increased, adhesion and growth of neurons also increased. This increase is seen both at early time points, 24 and 48 hours after plating, and at a later time point, 12 days after plating. These data suggest that this change in cell number is due to adhesion of cells and not cell death or cell loss from the gels. We hypothesize that either cells are not establishing appropriate numbers of lamellipodia and filopodia or not establishing these structures quickly enough for adhesion to occur, thus causing cell death or loss on softer substrates (17, 32, 92).

In contrast, the adhesion and growth of astrocytes differ when the cells are plated on soft gels. The number of neurons and astrocytes increased as initial plating density

increased only when the cells were grown on soft gels. In contrast, only neuronal and not astrocyte adhesion and growth increased as initial plating increased when cells were grown on hard gels. We conclude that adhesion and growth of astroctyes on hard gels does not change because a maximum threshold of adhesion may be reached, thus inhibiting additional astrocytes from binding to the surface of the hard substrate. Although astrocyte adhesion and growth are different on soft versus hard gels, increasing the initial plating density on soft gels allows astrocytes to reach similar densities as observed on hard gels.

The results from this study both corroborate and conflict with previously published reports. In contrast to our data, Georges *et al.* showed that neuronal adhesion is less when cells are plated on harder substrates versus softer substrates (30). In addition, a study from our laboratory showed that only pure neuronal or pure glial cultures, but not mixed cultures, show an increase in neuronal and glial adhesion and growth when stiffness increased (32). However, another study by our group showed that as substrate stiffness increases, the number of neurons in mixed cultures that adhere to and grow on hydrogels increases (31). Since initial plating density and cell types found in culture have effects on cellular adhesion and growth, differences in culture conditions may account for some of the differences seen in these reports.

Our results show that dendrite morphology is also affected by substrate stiffness. How can substrate stiffness mediate changes in dendrite branching? Astrocytes play key roles in regulating neurite outgrowth by providing neurotropic cues and support (120, 121) but do not appear to affect dendrite branching independently from stiffness in our studies. For neurons grown on soft substrates, the number of astrocytes increases as

plating density increases, but dendrite number and branching do not change. For neurons grown on hard gels, branching parameters change, but astrocyte number remains unchanged. The decreases for some branching parameters for neurons grown on hard gels as plating density increases could be due to a difference in neurotransmitter concentration. On the hard gels, neuronal number increased, and in turn, increased neuron number may result in increased release of neurotransmitters, such as glutamate. Glutamate reduces dendrite outgrowth and causes dendrite regression (122). At the synaptic cleft, astrocytes are responsible for the uptake of glutamate (123, 124). Since the number of astrocytes does not change but the number of neurons increases on hard substrates, there will be less glutamate uptake by astrocytes and more glutamate in the environment. Thus, dendrite parameters, including outgrowth may decrease because of the increase in glutamate.

Our studies are the first to report the separate effects of substrate stiffness and cell density on dendrite branching. Substrate stiffness affects dendrite patterning independently of culture density. We found that there are differences in the number and type of cells that adhere to and grow on gels of different compliances. Our data support previously published reports that show that neurite outgrowth increases when neurons are plated on substrates of increasing stiffness (31, 33). However, there are also conflicting reports that show that neurons grown on softer substrates have more dendrite branches than those grown on stiffer substrates (32, 53). Differences in these reports may be due to the differences in culture densities, animal source of cells, neuronal cell types, stiffness ranges, and/or culture ages (33). Taken together, these data strongly suggest that substrate

stiffness plays a greater role in determining the shape of the dendritic arbor than does cell density.

Chapter 2: Intracellular Cues : NOS1AP protein levels are specifically elevated in the prefrontal cortex of patients with schizophrenia.

INTRODUCTION

Schizophrenia is a chronic cognitive disorder that affects behavior and emotion (125). Schizophrenia is characterized by positive, negative, and cognitive symptoms (126). Positive symptoms include hallucinations, disorganized speech, and delusions (127), whereas negative symptoms include apathy and lack of emotions. Cognitive symptoms include attention and memory problems (128).

Genes involved in the regulation of recovery from ischemia-hypoxia and function of the vasculature are looked at as candidates for schizophrenia susceptibility. Nitric oxide synthase 1 (neuronal; nNOS) adaptor protein (NOS1AP), also termed carboxyl-terminal PDZ ligand of nNOS or CAPON, is a candidate for schizophrenia susceptibility because of its role in ischemia-hypoxia (68). Brzustowicz and colleagues recently identified significant linkage disequilibrium between schizophrenia and the gene for NOS1AP (68). More recently, they further isolated a single risk allele within this gene that is associated with schizophrenia (68, 129). Initially identified in rat, NOS1AP plays a role in the inhibition of glutamate neurotransmission via disruption of nNOS binding to both PSD-95 and PSD-93. This results in uncoupling of nNOS from the NMDA receptor, and ultimately, inhibition of receptor activation (66, 70, 130). Further studies using quantitative real-time PCR analysis of mRNA from human postmortem dorsolateral prefrontal cortex (DLPFC) reveal that expression of a newer shortened isoform of the NOS1AP gene is significantly increased in patients with schizophrenia or bipolar disorder (70). Taken together, these data provide a role for NOS1AP in glutamate neurotransmission and manifestation of schizophrenia, suggesting that elucidation of the NOS1AP signaling pathway in neurons may provide novel targets for treatment of

schizophrenia and related disorders. However, despite these recent reports establishing linkage between NOS1AP and schizophrenia, it is unknown whether NOS1AP protein expression is increased specifically in prefrontal cortical regions in patients with schizophrenia.

Currently, two NOS1AP protein isoforms have been identified (66, 70). The first isoform is a ten exon full-length mRNA transcript that encodes a 501 amino acid protein with two functional domains, amino-terminal phosphotyrosine-binding and carboxyl-terminal PDZ-binding domains. The second transcript contains the last two exons of the full-length isoform and encodes a 211 amino acid protein with a PDZ-binding domain. It is reported that the terminal 125 amino acids of the full-length NOS1AP protein are sufficient to bind the PDZ-domain of nNOS (66, 70, 131).

Previous data suggest that changes in gene expression in distinct cortical regions (i.e. Brodmann area 46; BA46 and Brodmann area 11; BA11) may influence the pathophysiology and progression of schizophrenia (132, 133). In the following study, we analyzed changes in NOS1AP protein expression in human postmortem cortex and cerebellum of patients diagnosed with schizophrenia and of unaffected patients. These data provide evidence of increased expression for specific isoforms of NOS1AP in BA46 and BA11 in brains from patients with schizophrenia when compared to unaffected patients. However, no significant changes in NOS1AP protein expression were noted in the cerebellum, medial temporal lobe (MTL), or occipital lobe (OL). These data support a role for NOS1AP in schizophrenia and suggest that targeted alterations in NOS1AP expression may provide additional intervention points for treating or managing this disorder.

MATERIALS AND METHODS

Human postmortem tissue samples

Human postmortem tissue samples from patients with schizophrenia (n=6) and unaffected control patients (n=6) were collected, sectioned, and uniformly dissected into specific brain regions by the Human Brain and Spinal Fluid Resource Center (Los Angeles, California, United States). Brain sections in regions BA46, BA11, cerebellum, MTL, and OL were analyzed. Information on patients is in **Table 2**.

Patient Number	Diagnosis	Age	Gender	Hemishphere	Approximate Date of Death
707	SCZ	28	Male	R	7/6/83
2211	SCZ	73	Male	R	8/5/93
2798	SCZ	57	Female	L	12/23/98
299	SCZ	53	Female	R	9/30/77
677	SCZ	20	Male	R	5/11/83
1651	SCZ	59	Male		6/28/90
3175	Control	54	Female	?	6/14/01
3216	Control	79	Male	?	4/22/02
3221	Control	90	Male	?	5/4/02
2852	Control	61	Female	L	11/12/98
2994	Control	43	Female	?	7/18/00
3132	Control	53	Male	L	2/16/01

Table 2. Demographic on Postmortem Samples.

Tissue preparation and immunoblotting

Upon receipt, samples were ground into a fine powder while still frozen using liquid nitrogen and a mortar and pestle. Tissue was then homogenized in ten times the equivalent volume per weight of TEE (25 mM Tris-HCl [pH 7.4], 1 mM EDTA, 1 mM EGTA, and 1 mM PMSF) using a serrated Teflon pestle. Twenty micrograms of protein were loaded and resolved on a 12% SDS polyacrylamide gel and transferred to polyvinylidene difluoride membrane (Immobilon P; Millipore, Billerica, Massachusetts, United States) in transfer buffer lacking SDS. Membranes were blocked for 60 minutes in blocking solution containing 2% BSA and 0.02% sodium azide in TBST (25mM Tris [pH 7.4], 3mM KCl, 140mM NaCl, and 0.05% Tween20) and probed overnight at 4°C with a 1:250 dilution in blocking solution of rabbit antibody to NOS1AP (Santa Cruz Biotechnology, Santa Cruz, California, United States; #R-300) as previously described (70). Blots were then probed with a 1:3000 dilution of secondary antibody coupled to horseradish peroxidase (Rockland Immunochemicals Inc., Gilbertsville, Pennsylvania, United States) for 45-60 minutes and visualized using Luminol/Enhancer Solution (Pierce, Rockford, Illinois, United States). For normalization to glyceraldehyde 3-phosphate dehydrogenase (GAPDH) protein expression, the same blots were probed with a 1:300-1:2000 dilution of mouse antibody to GAPDH (Chemicon; Millipore, Billerica, Massachusetts, United States).

Band intensity was quantified using Image Pro image analysis software (Media Cybernetics, Silver Spring, Maryland, United States) and relative intensities of NOS1AP bands were calculated and normalized to the GAPDH intensities as control (70).

Investigators were blinded to all subject information until after the statistical analyses were complete.

Statistical analysis

NOS1AP expression levels were determined based on chemiluminescent band intensity normalized to GAPDH band intensity. Normalized values for subjects with schizophrenia were averaged and compared to the average values for samples from the unaffected control patients within the same brain region. Student's t-tests were used to evaluate differences between the two groups in each brain region.

RESULTS

Immunoblotting was performed on postmortem tissue samples of patients diagnosed with schizophrenia and with samples from unaffected control patients to assess NOS1AP expression. Four or more of each sample type were collected and detected for NOS1AP and GAPDH. Band intensities were quantified for the three NOS1AP forms and normalized to GAPDH band intensity. Although protein concentration was standardized via a Bradford protein assay prior to analysis, samples were not entirely uniform, and thus, they were normalized to GAPDH expression as a second loading control. GAPDH was not uniform in samples, possibly due to protein degradation.

There have been at least three protein isoforms of NOS1AP in the brain detected by Western blotting (70). There are two short isoforms (S and S′; exons 9 -10) and one long form (L; exons 1-10) of NOS1AP. We performed densitometry on Western blots of brain extracts probed for these three isoforms individually and also analyzed the two

short forms together (S+S′). The regions of the brain we immunoblotted for NOS1AP expression were Brodmann's Area (BA) 46 and 11, the cerebellum, MTL and the OL.

Schizophrenia has been shown to be associated with changes predominantly in the DLPFC, also known as BA46, and the hippocampal region of the MTL (109). Moreover, we choose to run samples specifically from BA46 and BA11 because all three isoforms of NOS1AP have been identified in these regions in patients diagnosed with schizophrenia (70).

As previously reported, the short isoform of NOS1AP appears as a doublet in all blots (**Figures 17** and **18**) (70). In BA46 and BA11, there were several changes in NOS1AP protein expression. In BA46, NOS1AP-L, and NOS1AP-S increased significantly in individuals with schizophrenia. Moreover, NOS1AP-S′ tended to increase in patients with schizophrenia, which is marginally significant ($p=0.0502$). In addition, the combination of two short forms of NOS1AP also increased in patients with schizophrenia (**Figure 17 A** and **B**). BA11 results were slightly different from BA46. In this region, NOS1AP-L did not change in patients with schizophrenia; however NOS1AP-S increased in patients diagnosed with schizophrenia (**Figure 17 C** and **D**). The two short forms of NOS1AP together also increased in patients with schizophrenia (**Figure 17 C** and **D**).

Next, we analyzed samples from regions of the brain where changes in NOS1AP protein isoforms were not expected. We ran protein samples from the cerebellum, MTL, and OL regions of the brains. As predicted, these regions had no significant differences in protein expression of any isoform of NOS1AP (**Figure 18**).

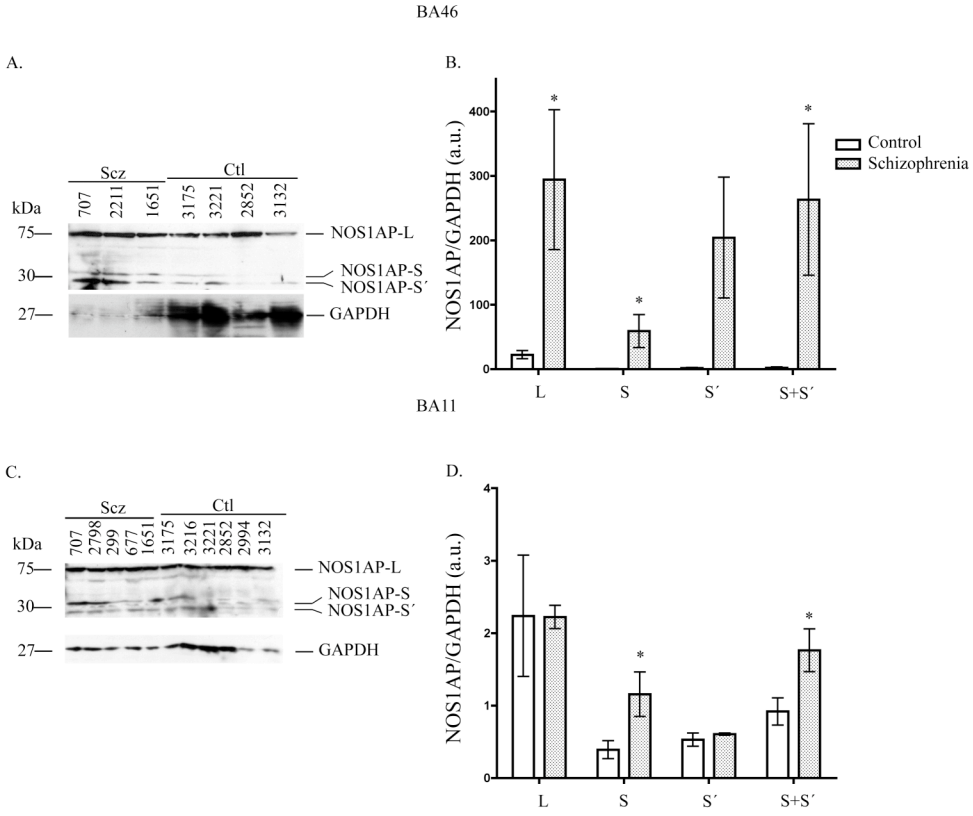

Figure 17. Postmortem tissue samples from BA 46 and 11 of patients diagnosed with schizophrenia and of unaffected control patients were analyzed via immunoblotting for the long and short isoforms of NOS1AP. (A) Immunoblot of protein samples extracted from BA46. (B) Densitometry analysis of image A. *p<0.05 determined by Student's t-test. (C) Immunoblot of protein samples extracted from BA11. (D) Densitometry analysis of image C. *p<0.05 determined by Student's t-test.

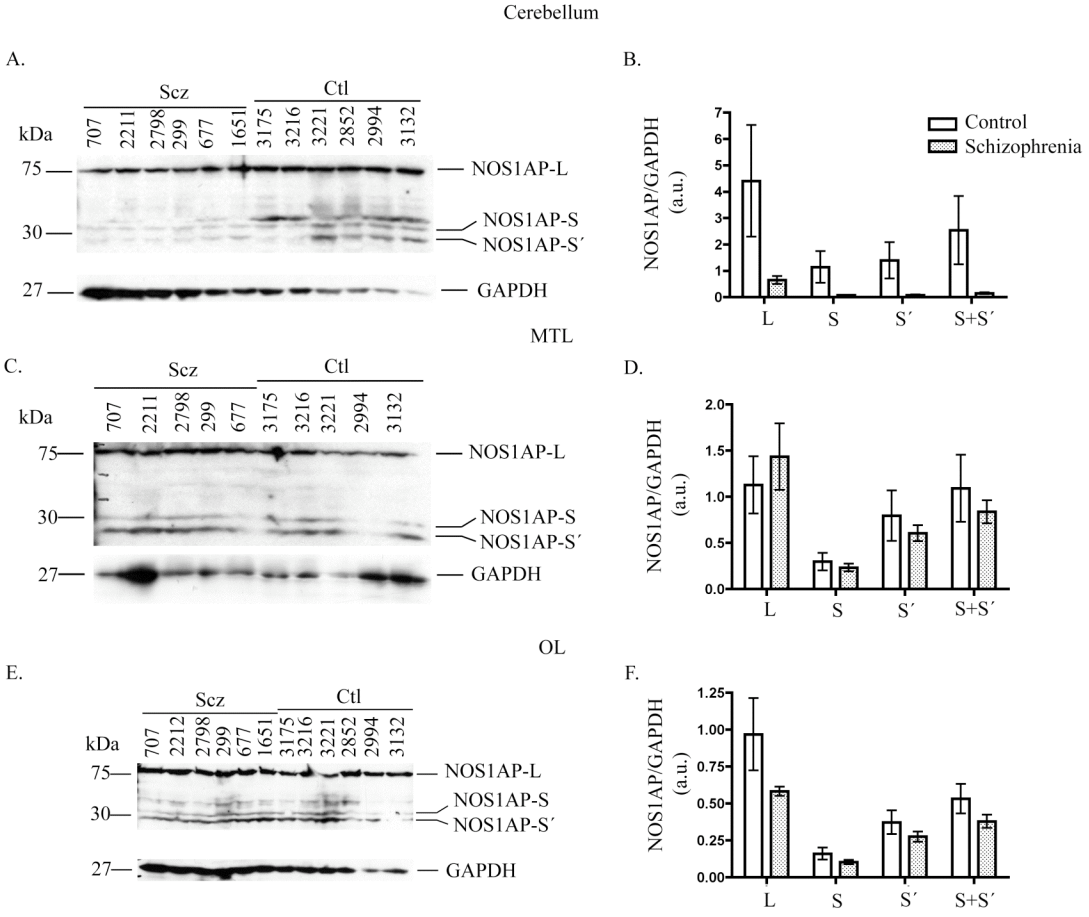

Figure 18. Postmortem tissue samples from cerebellum, MLT, and OL brain regions of patients diagnosed with schizophrenia and of unaffected control patients were analyzed via immunoblotting for the long and short isoforms of NOS1AP. (A) Immunoblot of protein samples extracted from cerebellum. (B) Densitometry analysis of image (C) Immunoblot of protein samples extracted from MLT. (D) Densitometry analysis of image C. (E) Immunoblot of protein samples extracted from OCL. (F) Densitometry analysis of image E.

DISCUSSION

NOS1AP and Brodmann area 46 and 11

In this study, we analyzed NOS1AP protein expression in several brain regions that may or may not have been previously reported to play a significant role in schizophrenia.

The cortex is divided into Brodmann areas**,** which are based on cytoarchitecture. BA19 and 11 were the first regions to show abnormalities in patients' diagnosed with schizophrenia (134, 135). Our data confirm increased levels of NOS1AP protein, both long and short form, in postmortem DLPFC tissue of patients diagnosed with schizophrenia, specifically in the BA46 and BA11 regions, when compared to unaffected patients. These results corroborate previous data where NOS1AP expression increased in BA46 of patients diagnosed with schizophrenia (70).

Our results are also consistent with previous reports implicating these regions in the etiology of schizophrenia. For example, previous reports from Thomas and colleague. examined expression of apolipoprotein D, a 29 kDa glycoprotein that exhibits increased expression in distinct CNS regions during various neurological disorders (136). They reported that apolipoprotein D expression is significantly and specifically increased in the BA46 and BA11 regions of the DLPFC in patients with schizophrenia. Another study examined the expression of apoliproprotein E, a 34 kDa lipid transporter that exhibit a change in allele frequencies in patients diagnosed with schizophrenia (137, 138). The expression of apolipoprotein E increased in the BA46 region for patients diagnosed with schizophrenia compared to unaffected patients (133, 139).

Further studies from Gupta and colleagues reported increased metabotropic glutamate receptor expression in several regions of the prefrontal cortex, including BA46 and BA11, in patients with schizophrenia (140). These data suggest that the reported increase may mediate a decrease in NMDA receptor activity since NOS1AP uncouples PSD-95 from nNOS, hence decreasing the amount of nNOS that may be activated by calcium influx by NMDA receptor activation (**Figure 19**). Thus, our data support the NMDA receptor hypofunction hypothesis and confirm the significance of the prefrontal cortex in the pathophysiology of schizophrenia.

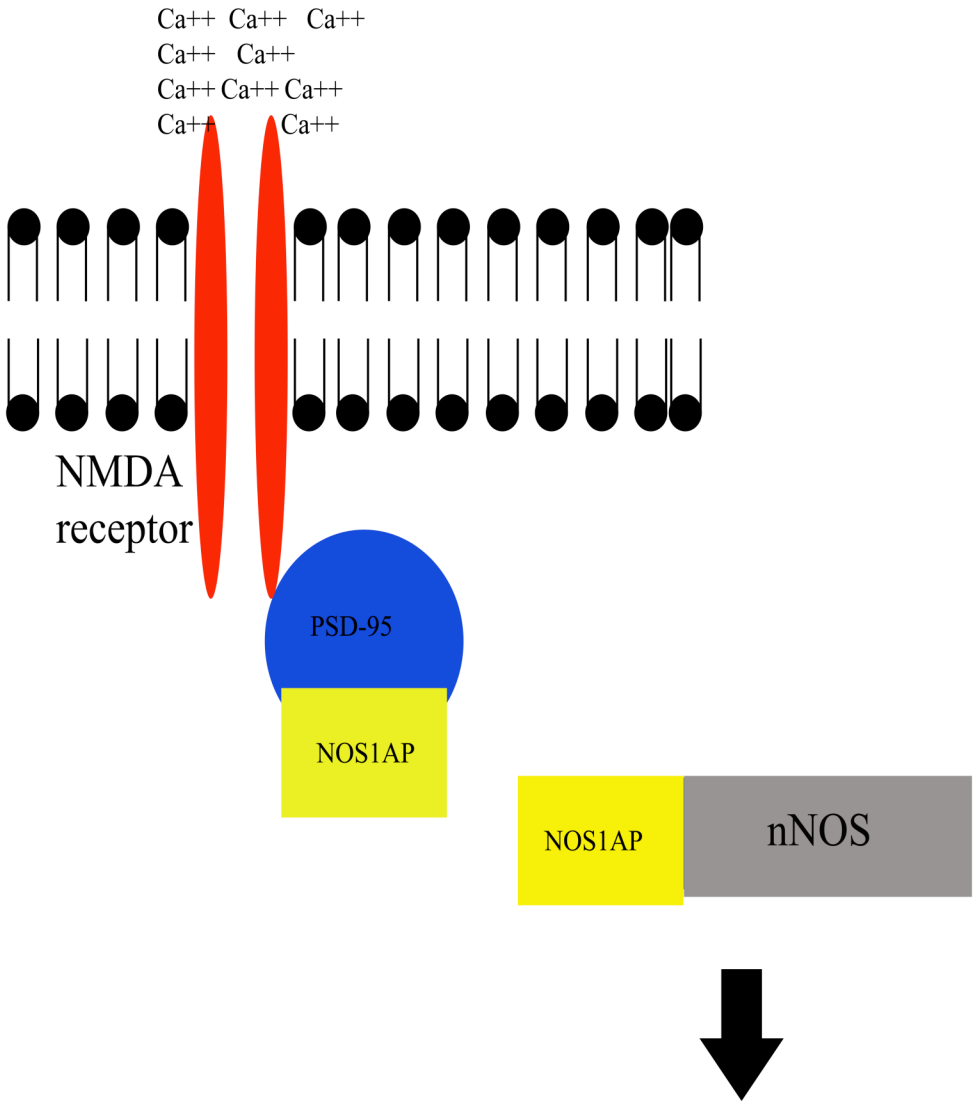

Figure 19. NMDA hypofuntion hypothesis.

NOS1AP and the cerebellum, medial temporal lobe, and occipital lobe

Additional analysis of NOS1AP expression reveals that no significant changes were evident in the cerebellum, MTL, or OL of patients with schizophrenia versus unaffected patients.

Patients diagnosed with schizophrenia show subtle abnormalities in motor and sensory skills and loss of cerebellum volume (141, 142). While some reports have indicated that schizophrenia may affect the cerebellum, the results are not as consistently observed as in other regions, namely the prefrontal cortex (143, 144). Thus, our data are consistent with studies reporting specific changes in DLPFC protein expression in schizophrenia, as we observed no significant changes in NOS1AP protein expression in cerebellum (140).

Strong evidence implicates the MTL in a range of mental illnesses, including schizophrenia (145, 146). According to MRI studies, patients diagnosed with schizophrenia have smaller MTLs (147-149). However, much of these data focused on neuronal changes specifically in the hippocampal region of the MTL (146, 150, 151). Our findings indicate that there were no significant differences in NOS1AP expression in the dissected MTL region from postmortem brain tissue in patients with schizophrenia and control patients. However, examination of the dissected region of MTL used in our analysis reveals that this section did not include hippocampal tissue. Additional analysis of NOS1AP expression in isolated postmortem hippocampus must be performed in order to determine whether NOS1AP is specifically upregulated in this region.

Patients diagnosed with schizophrenia have visual perception defects, such as hallucinations (152, 153). There are some published reports demonstrating irregularities

in the OL (154, 155). Our analysis of the OL region reveals no significant changes in NOS1AP protein expression in tissue from patients with schizophrenia versus unaffected patients. These results are consistent with previous reports documenting unaltered expression of schizophrenia-related proteins in the OL (156). Thus, only the DLPFC, hippocampus, and dorsal thalamus play roles in the manifestation of schizophrenia (109, 157).

In conclusion, results from this study indicate that NOS1AP protein levels are specifically elevated in the BA46 and BA11 regions of prefrontal cortex of patients with schizophrenia. These data suggest a role for NOS1AP in manifestation of schizophrenia. Further study of the molecular mechanisms responsible for this increase in NOS1AP expression and the downstream effects of this increase will provide insight into pathways responsible for the development of schizophrenia.

Conclusion

In this thesis, we address how extracellular and intracellular cues can affect neuronal morphology. We examined how changes in extracellular matrix stiffness, which may or may not be due to brain injury and disease, influences dendrite branching parameters. Moreover, we examined how NOS1AP, an intracellular protein, may be altered as a result of schizophrenia.

In Chapter 1, we examined the effects of extracellular matrix compliance on dendrite morphology in cultured hippocampal neurons. At an intermediate stiffness (8 kPa), dendrite branching peaks. Adhesion forces may be responsible for this phenomenon since adhesion molecules, such as laminin and neuronal-cadherin adhesion molecule (NCAM), have been shown to influence neurite outgrowth (158-160). On hard substrates, adhesion forces are too strong and inhibit dendrite branching, whereas on soft substrates, adhesion forces are weak and do not support dendrite branching. Thus, on the intermediate stiffness, the adhesion forces are optimal to allow maximum branching.

To verify this hypothesis, future experiments should be aimed towards measuring traction forces on compliant substrates. Previous studies have fabricated microposts to test for traction forces on adherent cells (161). Furthermore, magnetic beads have been attached to these microposts to allow a local, external force to be applied on attached cells (162). Thus, these two techniques may be used to further study the association between branching and adhesion of neuronal cells.

Future experiments using the above techniques should measure the amount of adhesion forces generated during active branching. Neurons can be plated on microposts without magnetic beads. The deflection of the posts at dendrite branch points can be

tabulated, and adhesion forces can be derived from post deflection. Next, adhesion markers, such as FAK, vincullin, N-cadherin, NCAM, and integrin, can be assessed by immunostaining to observe if more adhesion molecules are at branch points and post deflection sites. It is expected that more deflection will occur at branch points and more adhesion molecules will be at the deflection sites. Moreover, more deflection is expected to occur on harder gels, which would strengthen my hypothesis that stronger adhesion forces inhibit branching.

Related experiments include performing Western blotting of extracts from neurons grown on gels of various compliances. Blots would be probed and quantified for the adhesion molecules mentioned above. A greater number of adhesion molecules should be expressed on harder substrates. Higher expression on hard surfaces would confirm my hypothesis that strong adhesion forces inhibit dendrite branching.

Furthermore, neurons can be plated on microposts containing magnetic beads. At active stages of branching, a local force would be applied on the cell body, primary dendrites, and secondary dendrites. Branching should be observed at the origin of the applied force. If so, this experiment will show that forces are needed to generate a branch point.

As observed in Chapter 1b, in early stages of development (24 – 48 hrs after plating) and later stages of development (12 DIV), more neurons and mature astrocytes adhere on harder substrates. This difference in cell density between hard and soft substrates can influence branching parameters. We concluded that cell density effects are independent of substrate rigidity effects. In fact, the effect of substrate rigidity is dominant over cell density effects.

However, initial cell plating density still has an effect on branching: as density increases, branching decreases. This could be due to the glutamate concentration in the media. Future experiments would examine if glutamate is responsible for the decrease in branching. Experiments would include performing a Western blot for glutamate transporters in astrocyte cultures. Excitatory amino acid transporters 1 and 2 (EAAT1 and EAAT2; also known as GLAST and GLT-1, respectively) are receptors responsible for the primary uptake of glutamate in the central nervous system (163-165). To see if stiffness affects glutamate uptake, astrocytes will be plated on substrates of various compliances. Western blotting will be performed, and blots will be probed for changes in EAAT1 and EAAT2 expression among varying substrates. It is expected that the harder substrates will have less EAATs than the softer substrates. This would imply that the astrocytes are not taking up as much glutamate on harder substrates, and thus, neurons exhibit decreased branching.

Also in Chapter 1a, we examined the role that glutamate receptors play in dendrite branching on compliant substrates. We showed that NMDA and AMPA receptors play different roles in regulating dendrite branching of neurons grown on compliant substrates. On harder substrates, $\geq$2kPa, AMPA receptors play a role in dendritic arborization at all distances from the cell body. NMDA receptors play a role in dendritic arborization for a range of rigidities (1-25 kPa) but only at proximal and intermediate lengths from the cell body.

Future work will examine the mechanism of how AMPA and NMDA receptors are contributing to branching on compliant substrates. Differences in NMDA and AMPA receptor function could be due to differences in 1) receptor distribution, 2) roles in

adhesion, or 3) roles in dendrite branching. Future experiments would observe receptor distribution on various substrate rigidities by immunostaining of AMPA and NMDA receptors in neurons plated on various gels. Moreover, we would examine if glutamate receptors are working in conjunction with adhesion molecules to influence branching on compliant substrates. Adhesion proteins influence NMDA and AMPA receptor function and recruitment. NMDA receptors have been observed in complexes with adhesion molecules (166). Moreover, AMPA receptors interact with and perform reciprocal recruitment of N-cadherin (167, 168). Thus, the adhesion of hippocampal neurons to the substrate might be influencing the role of glutamate receptors in branching on compliant substrates. For these experiments, we would observe the co-localization of glutamate receptors with adhesion molecules.

To further understand the role that glutamate receptors play with adhesion molecules in the regulation of dendrite branching of neurons grown on substrates of different compliances, we would also take advantage of the micropost technique that was explained above. We would immunostain for AMPA and NMDA receptor subunits and observe if these receptors are located at points of branching and/or deflections of microposts. This experiment would determine if glutamate receptors are working with adhesion molecules to affect dendrite branching of neurons grown on compliant substrates.

We attempted to perform Western blotting for NMDA and AMPA receptors to observe their expression in neurons plated on substrates of various compliances. We probed for and quantitated different phosphorylated NR1 and GluR1 subunits and for total NR1 and GluR1 subunits. No changes in protein expression were observed for

phosphorylated or total subunits (data not shown). It is possible that other subunits, such as NR2, GluR2, GluR3 isoforms, are changing independent from the subunits we assayed for. Also, Western blotting might not be the appropriate experiment to determine the function of these receptors. In future experiments, we would perform surface immunostaining of glutamate receptors. It is possible that more receptors are expressed on the surface of neurons and contribute to the regulation of dendrite branching of neurons grown on compliant substrates.

Brain stiffness changes with injury, disease, and age. Future experiments will show how stiffness changes with age, injury, and disease *in vivo*. A study of human grey and white matter by Ehman and colleagues reported that stiffness of the brain does not change between the ages of 20-80 years of age for healthy patients (169). A caveat to this study is they did not examine the developing brain. Future experiments would include performing rheology studies on mouse brains of various ages, P1 to adulthood, to observe if changes in stiffness occur at extremely young ages on a global scale.

Traumatic brain injury changes the compliance of the brain, which may result in physiological changes in the cell. Scar tissue is less complaint than uninjured tissue (46, 49). Brain compression from brain injury increases brain compliance (170). Also, intracranial pressure due to brain injury also changes brain compliance (171). To observe how neurons are changing with injury, stretchable materials would be used to injure neurons. Atomic force microscopy would be performed to observe the change in the stiffness of the neuron at several locations: cell body, dendrite, axon, axonal terminal tips. These experiments would show how injury and age change neuronal stiffness.

Some compliance studies have been performed for injured and aging brains, but no studies have been identified for disease states, such as Alzheimer's and Parkinson's Disease. To study how disease affects the mechanical properties of the brain, future experiments would include the use of mouse models. Brains from mouse models of Alzheimer's Disease would be dissected, sectioned, and maintained in an isotonic buffer. Atomic force microscopy would be used to determine the stiffness of specific zones in and around an amlyoid plaque. Results would be compared to normal brains of the same background of mouse in the same area of the brain. Moreover, global measurements of the mouse brain would be acquired by rheology to determine the overall effect of the disease on the entire brain.

Lastly, in collaboration with the Brzustowicz laboratory and Dr. Norell Hadzimichalis, we examined the protein expression of three isoforms of NOS1AP in patients with schizophrenia and control patients. These protein isoforms were previously identified in the DLPFC of patients with schizophrenia, and they are genetically linked to schizophrenia (68, 70, 129). We found that expression of these isoforms of NOS1AP is increased only in the DLPFC region of the brain in patients with schizophrenia.

Further studies of the molecular mechanisms responsible for the increased NOS1AP expression, and the resultant downstream effects, will provide insight into pathways involved in the development of schizophrenia. We would perform Western blotting for quantifying NMDA receptors subunits to see if NMDA receptor expression corresponds to increased NOS1AP expression in patients with schizophrenia. Furthermore, we would determine whether different isoforms of NMDA subunits, such as

NR1, NR2A, and NR2A, are decreased in patients with schizophrenia, based on the NMDA hypofunction hypothesis.

We would also observe the effect of NOS1AP overexpression on NMDAR, nNOS, and PSD-95 receptor trafficking. We would transfect cortical neurons with constructs encoding NOS1AP and perform surface staining for NMDA receptor subunits. We would also immunostain for PSD-95 puncta and assess puncta size. We do not expect to see a change in trafficking of NMDAR subunits or PSD-95 because these are upstream of nNOS signaling.

To summarize, we show that extracellular and intracellular cues can affect the brain. Changes in extracellular matrix stiffness influence dendrite branching parameters. NOS1AP, an intracellular protein, may be involved in the manifestation of schizophrenia. Future experiments are needed to completely understand how the extracellular cues influence branching and how overexpression of NOS1AP creates a hypofunctioning NMDA receptor.

APPENDIX

Distance from Cell Body	E (kPa)	P Value	ANOVA followed by Dunnett's	Krustal Wallis followed by Dunn's
15	8	<0.05		X
21	8	<0.05		X
27	8	<0.05	X	
33	8	<0.01		X
39	8	<0.05	X	
45	8	<0.01		X
51	8	<0.001		X
57	8	<0.01		X
63	8	<0.01	X	
69	8	<0.01		X
75	8	<0.01		X
81	8	<0.05		X
87	8	<0.05		X
93	8	<0.05		X
99	8	<0.05		X
105	8	<0.05		X

Table 3. Statistics for neurons grown on 1 to 25 kPa gels and compared to neurons grown on 1 kPa gels.

Distance from Cell Body	CNQX Treatment	APV Treatment	P Value	ANOVA followed by Dunnett's	Krustal Wallis followed by Dunn's
15		X	<0.05	X	
21		X	<0.01	X	
27		X	<0.05	X	

Table 4. Statistics for CNQX or APV-treated neurons grown on 1 kPa hydrogels and compared to vehicle-treated control.

Distance from Cell Body	CNQX Treatment	APV Treatment	P Value		ANOVA followed by Dunnett's	Krustal Wallis followed by Dunn's
			CNQX	APV		
51	X		<0.05		X	
57	X		<0.05		X	
63	X		<0.05		X	
69	X		<0.01			X
75	X		<0.05		X	
81	X		<0.01			X
87	X		<0.01			X
93	X		<0.01			X
99	X	X	<0.001	<0.05		X
105	X		<0.001			X
111	X		<0.001			X
117	X		<0.01			X
123	X		<0.05			X
129	X		<0.05			X
135	X		<0.05			X
147	X		<0.05			X
153	X		<0.05			X
159	X		<0.05			X
165	X		<0.05			X

Table 5. Statistics for CNQX or APV-treated neurons grown on 2 kPa hydrogels and compared to vehicle-treated control.

Distance from Cell Body	CNQX Treatment	APV Treatment	P Value	ANOVA followed by Dunnett's	Krustal Wallis followed by Dunn's
63	X		<0.05		X
69	X		<0.05		X
75	X		<0.05		X
81		X	<0.01		X

Table 6. Statistics for CNQX or APV-treated neurons grown on 8 kPa hydrogels and compared to vehicle-treated control.

Distance from Cell Body	CNQX Treatment	APV Treatment	P Value		ANOVA followed by Dunnett's	Krustal Wallis followed by Dunn's
9	X	X	<0.05			X
15	X	X	<0.01	<0.05		X
21	X	X	<0.01			X
27	X	X	<0.01		X	
33	X		<0.01			X
39	X	X	<0.01	<0.05	X	
45	X	X	<0.05		X	
51	X	X	<0.05		X	
57	X	X	<0.05			X

Table 7. Statistics for CNQX or APV-treated neurons grown on 25 kPa hydrogels and compared to vehicle-treated control.

Distance from Cell Body	E (kPa)	P Value	ANOVA followed by Dunnett's	Krustal Wallis followed by Dunn's
45	25	<0.05		X
81	25	<0.05		X
87	25	<0.05	X	
93	25	<0.01		X
99	25	<0.05	X	
105	25	<0.05		X
111	25	<0.05		X
135	8; 25	<0.05		X

Table 8. Statistics for CNQX-treated neurons grown on 1 to 25 kPa gels and compared to neurons grown on 1 kPa gels.

Distance from Soma (μm)	P Value for 80,000 cells/cm cells/cm^2	P Value for 100,000 cells/cm^2	ANOVA followed by Dunnett's Multiple Comparisons Test	Krustal Wallis followed by Dunn's Multiple Comparison
9	<0.01	<0.01	X	
15	<0.01	<0.01	X	
21		<0.01		X
27		<0.01		X
33	<0.05	<0.01	X	
39		<0.05	X	

Table 9. p values for distances from the soma (Sholl analysis) for neurons grown on hard gels at different initial plating densities versus 50,000 cells/cm^2.

Distance from Soma (μm)	P Value	Mann Whitney Test	Student's t Test
9	<0.0001	X	
15	<0.0001	X	
21	<0.0001	X	
27	<0.0001	X	
33	<0.0001	X	
39	<0.0001	X	
45	<0.0001	X	
51	<0.0001	X	
57	<0.0001	X	
63	<0.01	X	
69	<0.05	X	
75	<0.05	X	
81	<0.05	X	
87	0.0997	X	
93	0.0571	X	

Table 10. p values for distances from the soma (Sholl analysis) for neurons grown on soft vs. hard gels at an initial plating density of 50,000 cells/cm^2.

Distance from Soma (μm)	P Value	Mann Whitney Test	Student's t Test
21	<0.05	X	
27	<0.01		X
33	<0.01		X
39	<0.01		X
45	<0.01		X
51	<0.01		X
57	<0.05		X
63	<0.05	X	
69	<0.05	X	
75	<0.01	X	
81	<0.05	X	
87	<0.05	X	
93	<0.05	X	
99	<0.05	X	
105	<0.05	X	
111	<0.05	X	
117	<0.01	X	
123	<0.05	X	
129	0.059	X	

135	0.0845	X	
141	<0.05	X	

Table 11. p values for distances from the soma (Sholl analysis) for neurons grown on soft vs. hard gels at an initial plating density of 80,000 cells/cm^2.

Distance from Soma (μm)	P Value	Mann Whitney Test	Student's t Test
9	<0.05	X	
15	<0.05	X	
27	<0.05	X	
33	0.0742	X	
39	<0.05	X	
51	<0.01	X	
57	<0.01	X	
63	<0.01	X	
69	<0.05	X	
75	<0.05	X	

Table 12. p values for distances from the soma (Sholl analysis) for neurons grown on soft vs. hard gels at an initial plating density of 100,000 cells/cm^2.

BIBLIOGRAPHY

1. Carrel, D., Y. Du, D. Komlos, N. M. Hadzimichalis, M. Kwon, B. Wang, L. M. Brzustowicz, and B. L. Firestein. 2009. NOS1AP regulates dendrite patterning of hippocampal neurons through a carboxypeptidase E-mediated pathway. J Neurosci 29:8248-8258.

2. Eriksson, P. S., E. Perfilieva, T. Bjork-Eriksson, A. M. Alborn, C. Nordborg, D. A. Peterson, and F. H. Gage. 1998. Neurogenesis in the adult human hippocampus. Nat Med 4:1313-1317.

3. Doetsch, F., and A. Alvarez-Buylla. 1996. Network of tangential pathways for neuronal migration in adult mammalian brain. Proc Natl Acad Sci U S A 93:14895-14900.

4. Cameron, H. A., C. S. Woolley, B. S. McEwen, and E. Gould. 1993. Differentiation of newly born neurons and glia in the dentate gyrus of the adult rat. Neuroscience 56:337-344.

5. Kaplan, M. S., and J. W. Hinds. 1977. Neurogenesis in the adult rat: electron microscopic analysis of light radioautographs. Science 197:1092-1094.

6. Altman, J. 1969. Autoradiographic and histological studies of postnatal neurogenesis. 3. Dating the time of production and onset of differentiation of cerebellar microneurons in rats. J Comp Neurol 136:269-293.

7. Bremner, J. D., B. Elzinga, C. Schmahl, and E. Vermetten. 2008. Structural and functional plasticity of the human brain in posttraumatic stress disorder. Prog Brain Res 167:171-186.

8. Martinez-Tellez, R. I., E. Hernandez-Torres, C. Gamboa, and G. Flores. 2009. Prenatal stress alters spine density and dendritic length of nucleus accumbens and hippocampus neurons in rat offspring. Synapse 63:794-804.

9. McEwen, B. S., and A. M. Magarinos. 2001. Stress and hippocampal plasticity: implications for the pathophysiology of affective disorders. Hum Psychopharmacol 16:S7-S19.

10. Malberg, J. E., A. J. Eisch, E. J. Nestler, and R. S. Duman. 2000. Chronic antidepressant treatment increases neurogenesis in adult rat hippocampus. J Neurosci 20:9104-9110.

11. Kodama, M., T. Fujioka, and R. S. Duman. 2004. Chronic olanzapine or fluoxetine administration increases cell proliferation in hippocampus and prefrontal cortex of adult rat. Biol Psychiatry 56:570-580.

12. Duman, R. S., S. Nakagawa, and J. Malberg. 2001. Regulation of adult neurogenesis by antidepressant treatment. Neuropsychopharmacology 25:836-844.

13. Duman, R. S., J. Malberg, and S. Nakagawa. 2001. Regulation of adult neurogenesis by psychotropic drugs and stress. J Pharmacol Exp Ther 299:401-407.

14. Masland, R. H. 2004. Neuronal cell types. Curr Biol 14:R497-500.

15. Zoghbi, H. Y. 2003. Postnatal neurodevelopmental disorders: meeting at the synapse? Science 302:826-830.

16. Harrison, P. J. 2004. The hippocampus in schizophrenia: a review of the neuropathological evidence and its pathophysiological implications. Psychopharmacology (Berl) 174:151-162.

17. Dotti, C. G., C. A. Sullivan, and G. A. Banker. 1988. The establishment of polarity by hippocampal neurons in culture. J Neurosci 8:1454-1468.

18. Akum, B. F., M. Chen, S. I. Gunderson, G. M. Riefler, M. M. Scerri-Hansen, and B. L. Firestein. 2004. Cypin regulates dendrite patterning in hippocampal neurons by promoting microtubule assembly. Nat Neurosci 7:145-152.

19. McAllister, A. K., L. C. Katz, and D. C. Lo. 1997. Opposing roles for endogenous BDNF and NT-3 in regulating cortical dendritic growth. Neuron 18:767-778.

20. McAllister, A. K., D. C. Lo, and L. C. Katz. 1995. Neurotrophins regulate dendritic growth in developing visual cortex. Neuron 15:791-803.

21. Baker, R. E., P. A. Dijkhuizen, J. Van Pelt, and J. Verhaagen. 1998. Growth of pyramidal, but not non-pyramidal, dendrites in long-term organotypic explants of neonatal rat neocortex chronically exposed to neurotrophin-3. Eur J Neurosci 10:1037-1044.

22. Horch, H. W., A. Kruttgen, S. D. Portbury, and L. C. Katz. 1999. Destabilization of cortical dendrites and spines by BDNF. Neuron 23:353-364.

23. Horch, H. W., and L. C. Katz. 2002. BDNF release from single cells elicits local dendritic growth in nearby neurons. Nat Neurosci 5:1177-1184.

24. Liu, X., M. L. Robinson, A. M. Schreiber, V. Wu, M. M. Lavail, J. Cang, and D. R. Copenhagen. 2009. Regulation of neonatal development of retinal ganglion cell dendrites by neurotrophin-3 overexpression. J Comp Neurol 514:449-458.

25. Reist, N. E., M. J. Werle, and U. J. McMahan. 1992. Agrin released by motor neurons induces the aggregation of acetylcholine receptors at neuromuscular junctions. Neuron 8:865-868.

26. Mantych, K. B., and A. Ferreira. 2001. Agrin differentially regulates the rates of axonal and dendritic elongation in cultured hippocampal neurons. J Neurosci 21:6802-6809.

27. D'Arcangelo, G. 2006. Reelin mouse mutants as models of cortical development disorders. Epilepsy Behav 8:81-90.

28. Chen, M., K. G. Lucas, B. F. Akum, G. Balasingam, T. M. Stawicki, J. M. Provost, G. M. Riefler, R. J. Jornsten, and B. L. Firestein. 2005. A novel role for snapin in dendrite patterning: interaction with cypin. Mol Biol Cell 16:5103-5114.

29. Charych, E. I., B. F. Akum, J. S. Goldberg, R. J. Jornsten, C. Rongo, J. Q. Zheng, and B. L. Firestein. 2006. Activity-independent regulation of dendrite patterning by postsynaptic density protein PSD-95. J Neurosci 26:10164-10176.

30. Georges, P. C., W. J. Miller, D. F. Meaney, E. S. Sawyer, and P. A. Janmey. 2006. Matrices with compliance comparable to that of brain tissue select neuronal over glial growth in mixed cortical cultures. Biophys J 90:3012-3018.

31. Jiang, F. X., B. Yurke, B. L. Firestein, and N. A. Langrana. 2008. Neurite outgrowth on a DNA crosslinked hydrogel with tunable stiffnesses. Annals of Biomedical Engineering 36:1565-1579.

32. Jiang, X., P. C. Georges, B. Li, Y. Du, M. K. Kutzing, M. L. Previtera, N. A. Langrana, and B. L. Firestein. 2007. Cell Growth in Response to Mechanical Stiffness is Affected by Neuron-Astroglia Interactions. The Open Neuroscience Journal 1:7-14.

33. Leach, J. B., X. Q. Brown, J. G. Jacot, P. A. Dimilla, and J. Y. Wong. 2007. Neurite outgrowth and branching of PC12 cells on very soft substrates sharply decreases below a threshold of substrate rigidity. J Neural Eng 4:26-34.

34. Prietsch, S. O., G. B. Fischer, J. A. Cesar, B. S. Lempek, L. V. Barbosa, Jr., L. Zogbi, O. C. Cardoso, and A. M. Santos. 2003. [Respiratory illnesses in children younger than 5 years of age in southern Brazil: the influence of the home environment]. Rev Panam Salud Publica 13:303-310.

35. Armstrong, D., J. K. Dunn, B. Antalffy, and R. Trivedi. 1995. Selective dendritic alterations in the cortex of Rett syndrome. J Neuropathol Exp Neurol 54:195-201.

36. Multani, P., R. H. Myers, H. W. Blume, D. L. Schomer, and A. Sotrel. 1994. Neocortical dendritic pathology in human partial epilepsy: a quantitative Golgi study. Epilepsia 35:728-736.

37. Moolman, D. L., O. V. Vitolo, J. P. Vonsattel, and M. L. Shelanski. 2004. Dendrite and dendritic spine alterations in Alzheimer models. J Neurocytol 33:377-387.

38. McNeill, T. H., S. A. Brown, J. A. Rafols, and I. Shoulson. 1988. Atrophy of medium spiny I striatal dendrites in advanced Parkinson's disease. Brain Res 455:148-152.

39. Scott, S. A. 1993. Dendritic atrophy and remodeling of amygdaloid neurons in Alzheimer's disease. Dementia 4:264-272.

40. Scheibel, A. B. 1979. Dendritic changes in senile and presenile dementias. Res Publ Assoc Res Nerv Ment Dis 57:107-124.

41. Scheibel, A. B., and U. Tomiyasu. 1978. Dendritic sprouting in Alzheimer's presenile dementia. Exp Neurol 60:1-8.

42. Sgobio, C., A. Trabalza, A. Spalloni, C. Zona, I. Carunchio, P. Longone, and M. Ammassari-Teule. 2008. Abnormal medial prefrontal cortex connectivity and defective fear extinction in the presymptomatic G93A SOD1 mouse model of ALS. Genes Brain Behav 7:427-434.

43. Marmarou, A., A. L. Maset, J. D. Ward, S. Choi, D. Brooks, H. A. Lutz, R. J. Moulton, J. P. Muizelaar, A. DeSalles, and H. F. Young. 1987. Contribution of CSF and vascular factors to elevation of ICP in severely head-injured patients. J Neurosurg 66:883-890.

44. Miller, W. J., I. Leventhal, D. Scarsella, P. G. Haydon, P. Janmey, and D. F. Meaney. 2009. Mechanically induced reactive gliosis causes ATP-mediated alterations in astrocyte stiffness. J Neurotrauma 26:789-797.

45. Manwaring, P., D. Wichern, M. Manwaring, J. Manwaring, and K. Manwaring. 2004. A signal analysis algorithm for determining brain compliance non-invasively. Conf Proc IEEE Eng Med Biol Soc 1:353-356.

46. Hertegard, S., A. Dahlqvist, and E. Goodyer. 2006. Viscoelastic measurements after vocal fold scarring in rabbits--short-term results after hyaluronan injection. Acta Otolaryngol 126:758-763.

47. Hertegard, S., J. Cedervall, B. Svensson, K. Forsberg, F. H. Maurer, D. Vidovska, P. Olivius, L. Ahrlund-Richter, and K. Le Blanc. 2006. Viscoelastic and histologic properties in scarred rabbit vocal folds after mesenchymal stem cell injection. Laryngoscope 116:1248-1254.

48. Rousseau, B., J. Sohn, D. W. Montequin, I. Tateya, and D. M. Bless. 2004. Functional outcomes of reduced hyaluronan in acute vocal fold scar. Ann Otol Rhinol Laryngol 113:767-776.

49. Corr, D. T., C. L. Gallant-Behm, N. G. Shrive, and D. A. Hart. 2009. Biomechanical behavior of scar tissue and uninjured skin in a porcine model. Wound Repair Regen 17:250-259.

50. Pelham, R. J., Jr., and Y. Wang. 1997. Cell locomotion and focal adhesions are regulated by substrate flexibility. Proc Natl Acad Sci U S A 94:13661-13665.

51. Yeung, T., P. C. Georges, L. A. Flanagan, B. Marg, M. Ortiz, M. Funaki, N. Zahir, W. Ming, V. Weaver, and P. A. Janmey. 2005. Effects of substrate stiffness on cell morphology, cytoskeletal structure, and adhesion. Cell Motil Cytoskeleton 60:24-34.

52. Georges, P. C., and P. A. Janmey. 2005. Cell type-specific response to growth on soft materials. J Appl Physiol 98:1547-1553.

53. Flanagan, L. A., Y. E. Ju, B. Marg, M. Osterfield, and P. A. Janmey. 2002. Neurite branching on deformable substrates. Neuroreport 13:2411-2415.

54. McKegney, M., I. Taggart, and M. H. Grant. 2001. The influence of crosslinking agents and diamines on the pore size, morphology and the biological stability of collagen sponges and their effect on cell penetration through the sponge matrix. J Mater Sci Mater Med 12:833-844.

55. Garthwaite, J., S. L. Charles, and R. Chess-Williams. 1988. Endothelium-derived relaxing factor release on activation of NMDA receptors suggests role as intercellular messenger in the brain. Nature 336:385-388.

56. Bredt, D. S., and S. H. Snyder. 1989. Nitric oxide mediates glutamate-linked enhancement of cGMP levels in the cerebellum. Proc Natl Acad Sci U S A 86:9030-9033.

57. Knowles, R. G., M. Palacios, R. M. Palmer, and S. Moncada. 1989. Formation of nitric oxide from L-arginine in the central nervous system: a transduction mechanism for stimulation of the soluble guanylate cyclase. Proc Natl Acad Sci U S A 86:5159-5162.

58. Aquilano, K., S. Baldelli, G. Rotilio, and M. R. Ciriolo. 2008. Role of nitric oxide synthases in Parkinson's disease: a review on the antioxidant and anti-inflammatory activity of polyphenols. Neurochem Res 33:2416-2426.

59. Joca, S. R., and F. S. Guimaraes. 2006. Inhibition of neuronal nitric oxide synthase in the rat hippocampus induces antidepressant-like effects. Psychopharmacology (Berl) 185:298-305.

60. Huang, P. L., T. M. Dawson, D. S. Bredt, S. H. Snyder, and M. C. Fishman. 1993. Targeted disruption of the neuronal nitric oxide synthase gene. Cell 75:1273-1286.

61. Tanda, K., A. Nishi, N. Matsuo, K. Nakanishi, N. Yamasaki, T. Sugimoto, K. Toyama, K. Takao, and T. Miyakawa. 2009. Abnormal social behavior, hyperactivity, impaired remote spatial memory, and increased D1-mediated dopaminergic signaling in neuronal nitric oxide synthase knockout mice. Mol Brain 2:19.

62. Brenman, J. E., D. S. Chao, S. H. Gee, A. W. McGee, S. E. Craven, D. R. Santillano, Z. Wu, F. Huang, H. Xia, M. F. Peters, S. C. Froehner, and D. S. Bredt. 1996. Interaction of nitric oxide synthase with the postsynaptic density protein PSD-95 and alpha1-syntrophin mediated by PDZ domains. Cell 84:757-767.

63. MacDermott, A. B., M. L. Mayer, G. L. Westbrook, S. J. Smith, and J. L. Barker. 1986. NMDA-receptor activation increases cytoplasmic calcium concentration in cultured spinal cord neurones. Nature 321:519-522.

64. Cho, K. O., C. A. Hunt, and M. B. Kennedy. 1992. The rat brain postsynaptic density fraction contains a homolog of the Drosophila discs-large tumor suppressor protein. Neuron 9:929-942.

65. Ponting, C. P., and C. Phillips. 1995. DHR domains in syntrophins, neuronal NO synthases and other intracellular proteins. Trends Biochem Sci 20:102-103.

66. Jaffrey, S. R., A. M. Snowman, M. J. Eliasson, N. A. Cohen, and S. H. Snyder. 1998. CAPON: a protein associated with neuronal nitric oxide synthase that regulates its interactions with PSD95. Neuron 20:115-124.

67. Fang, M., S. R. Jaffrey, A. Sawa, K. Ye, X. Luo, and S. H. Snyder. 2000. Dexras1: a G protein specifically coupled to neuronal nitric oxide synthase via CAPON. Neuron 28:183-193.

68. Brzustowicz, L. M., J. Simone, P. Mohseni, J. E. Hayter, K. A. Hodgkinson, E. W. Chow, and A. S. Bassett. 2004. Linkage disequilibrium mapping of schizophrenia susceptibility to the CAPON region of chromosome 1q22. Am J Hum Genet 74:1057-1063.

69. McGuffin, P., P. Asherson, M. Owen, and A. Farmer. 1994. The strength of the genetic effect. Is there room for an environmental influence in the aetiology of schizophrenia? Br J Psychiatry 164:593-599.

70. Xu, B., N. Wratten, E. I. Charych, S. Buyske, B. L. Firestein, and L. M. Brzustowicz. 2005. Increased expression in dorsolateral prefrontal cortex of CAPON in schizophrenia and bipolar disorder. PLoS Med 2:e263.

71. Willits, R. K., and S. L. Skornia. 2004. Effect of collagen gel stiffness on neurite extension. J Biomater Sci Polym Ed 15:1521-1531.

72. Cullen, D. K., M. C. Lessing, and M. C. LaPlaca. 2007. Collagen-dependent neurite outgrowth and response to dynamic deformation in three-dimensional neuronal cultures. Ann Biomed Eng 35:835-846.

73. Wang, Y. L., and R. J. Pelham, Jr. 1998. Preparation of a flexible, porous polyacrylamide substrate for mechanical studies of cultured cells. Methods Enzymol 298:489-496.

74. Firestein, B. L., J. E. Brenman, C. Aoki, A. M. Sanchez-Perez, A. E. El-Husseini, and D. S. Bredt. 1999. Cypin: a cytosolic regulator of PSD-95 postsynaptic targeting. Neuron 24:659-672.

75. Xia, Z., H. Dudek, C. K. Miranti, and M. E. Greenberg. 1996. Calcium influx via the NMDA receptor induces immediate early gene transcription by a MAP kinase/ERK-dependent mechanism. J Neurosci 16:5425-5436.

76. Bonni, A., D. D. Ginty, H. Dudek, and M. E. Greenberg. 1995. Serine 133-phosphorylated CREB induces transcription via a cooperative mechanism that may confer specificity to neurotrophin signals. Mol Cell Neurosci 6:168-183.

77. Nikolic, M., H. Dudek, Y. T. Kwon, Y. F. Ramos, and L. H. Tsai. 1996. The cdk5/p35 kinase is essential for neurite outgrowth during neuronal differentiation. Genes Dev 10:816-825.

78. Dudek, H., S. R. Datta, T. F. Franke, M. J. Birnbaum, R. Yao, G. M. Cooper, R. A. Segal, D. R. Kaplan, and M. E. Greenberg. 1997. Regulation of neuronal survival by the serine-threonine protein kinase Akt. Science 275:661-665.

79. Horwitz, B. 1981. Neuronal plasticity: how changes in dendritic architecture can affect the spread of postsynaptic potentials. Brain Res 224:412-418.

80. Vaughn, J. E., R. P. Barber, and T. J. Sims. 1988. Dendritic development and preferential growth into synaptogenic fields: a quantitative study of Golgi-impregnated spinal motor neurons. Synapse 2:69-78.

81. Peacock, J. H., D. F. Rush, and L. H. Mathers. 1979. Morphology of dissociated hippocampal cultures from fetal mice. Brain Res 169:231-246.

82. Cline, H. T., and M. Constantine-Paton. 1990. NMDA receptor agonist and antagonists alter retinal ganglion cell arbor structure in the developing frog retinotectal projection. J Neurosci 10:1197-1216.

83. Cline, H. T., E. A. Debski, and M. Constantine-Paton. 1990. The role of the NMDA receptor in the development of the frog visual system. Adv Exp Med Biol 268:197-203.

84. Cline, H. T., and M. Constantine-Paton. 1989. NMDA receptor antagonists disrupt the retinotectal topographic map. Neuron 3:413-426.

85. Hirai, H., and T. Launey. 2000. The regulatory connection between the activity of granule cell NMDA receptors and dendritic differentiation of cerebellar Purkinje cells. J Neurosci 20:5217-5224.

86. Li, Z., L. Van Aelst, and H. T. Cline. 2000. Rho GTPases regulate distinct aspects of dendritic arbor growth in Xenopus central neurons in vivo. Nat Neurosci 3:217-225.

87. Heng, J. E., D. Zurakowski, C. K. Vorwerk, C. L. Grosskreutz, and E. B. Dreyer. 1999. Cation channel control of neurite morphology. Brain Res Dev Brain Res 113:67-73.

88. Rajan, I., and H. T. Cline. 1998. Glutamate receptor activity is required for normal development of tectal cell dendrites in vivo. J Neurosci 18:7836-7846.

89. Rajan, I., S. Witte, and H. T. Cline. 1999. NMDA receptor activity stabilizes presynaptic retinotectal axons and postsynaptic optic tectal cell dendrites in vivo. J Neurobiol 38:357-368.

90. Kostic, A., J. Sap, and M. P. Sheetz. 2007. RPTPalpha is required for rigidity-dependent inhibition of extension and differentiation of hippocampal neurons. J Cell Sci 120:3895-3904.

91. Tija, J., and P. Moghe. 2002. "Dynamic," Cell Internalizable, Ligand Microinterfaces. Tissue Engineering 8:247-261.

92. Chan, C. E., and D. J. Odde. 2008. Traction dynamics of filopodia on compliant substrates. Science 322:1687-1691.

93. Chamak, B., and A. Prochiantz. 1989. Influence of extracellular matrix proteins on the expression of neuronal polarity. Development 106:483-491.

94. Monnerie, H., S. Shashidhara, and P. D. Le Roux. 2003. Decreased dendrite growth from cultured mouse cortical neurons surviving excitotoxic activation of alpha-amino-3-hydroxy-5-methyl-4-isoxazole propionate/kainate receptors. Neurosci Lett 345:182-186.

95. Luthi, A., L. Schwyzer, J. M. Mateos, B. H. Gahwiler, and R. A. McKinney. 2001. NMDA receptor activation limits the number of synaptic connections during hippocampal development. Nat Neurosci 4:1102-1107.

96. Hof, P. R., P. Vissavajjhala, R. E. Rosenthal, G. Fiskum, and J. H. Morrison. 1996. Distribution of glutamate receptor subunit proteins GluR2(4), GluR5/6/7, and NMDAR1 in the canine and primate cerebral cortex: a comparative immunohistochemical analysis. Brain Res 723:77-89.

97. Piccini, A., and R. Malinow. 2002. Critical postsynaptic density 95/disc large/zonula occludens-1 interactions by glutamate receptor 1 (GluR1) and GluR2 required at different subcellular sites. J Neurosci 22:5387-5392.

98. Earnshaw, B. A., and P. C. Bressloff. 2006. Biophysical model of AMPA receptor trafficking and its regulation during long-term potentiation/long-term depression. J Neurosci 26:12362-12373.

99. Jakobs, T. C., A. Koizumi, and R. H. Masland. 2008. The spatial distribution of glutamatergic inputs to dendrites of retinal ganglion cells. J Comp Neurol 510:221-236.

100. Piccini, P. 2002. Neuropsychological performance and integrated evaluation for disabled people using Virtual Reality: integrated VR profile. Stud Health Technol Inform 85:348-354.

101. Kramar, E. A., J. A. Bernard, C. M. Gall, and G. Lynch. 2003. Integrins modulate fast excitatory transmission at hippocampal synapses. J Biol Chem 278:10722-10730.

102. Bernard-Trifilo, J. A., E. A. Kramar, R. Torp, C. Y. Lin, E. A. Pineda, G. Lynch, and C. M. Gall. 2005. Integrin signaling cascades are operational in adult hippocampal synapses and modulate NMDA receptor physiology. J Neurochem 93:834-849.

103. Lin, B., A. C. Arai, G. Lynch, and C. M. Gall. 2003. Integrins regulate NMDA receptor-mediated synaptic currents. J Neurophysiol 89:2874-2878.

104. Juhasz, G., G. Vass, Z. Bozso, D. Budai, B. Penke, and V. Szegedi. 2008. Integrin activation modulates NMDA and AMPA receptor function of CA1 cells in a dose-related fashion in vivo. Brain Res 1233:20-26.

105. Jan, Y. N., and L. Y. Jan. 2003. The control of dendrite development. Neuron 40:229-242.

106. Spruston, N. 2008. Pyramidal neurons: dendritic structure and synaptic integration. Nat Rev Neurosci 9:206-221.

107. Landgraf, M., and J. F. Evers. 2005. Control of dendritic diversity. Curr Opin Cell Biol 17:690-696.

108. Anderton, B. H., L. Callahan, P. Coleman, P. Davies, D. Flood, G. A. Jicha, T. Ohm, and C. Weaver. 1998. Dendritic changes in Alzheimer's disease and factors that may underlie these changes. Prog Neurobiol 55:595-609.

109. Harrison, P. J. 1999. The neuropathology of schizophrenia. A critical review of the data and their interpretation. Brain 122 (Pt 4):593-624.

110. Georges, P. C., N. M. Hadzimichalis, E. S. Sweet, and B. L. Firestein. 2008. The yin-yang of dendrite morphology: unity of actin and microtubules. Mol Neurobiol 38:270-284.

111. Vessey, J. P., and D. Karra. 2007. More than just synaptic building blocks: scaffolding proteins of the post-synaptic density regulate dendritic patterning. J Neurochem 102:324-332.

112. Cove, J., P. Blinder, E. Abi-Jaoude, M. Lafreniere-Roula, L. Devroye, and D. Baranes. 2006. Growth of neurites toward neurite- neurite contact sites increases synaptic clustering and secretion and is regulated by synaptic activity. Cereb Cortex 16:83-92.

113. Cove, J., P. Blinder, and D. Baranes. 2009. Contacts among non-sister dendritic branches at bifurcations shape neighboring dendrites and pattern their synaptic inputs. Brain Res 1251:30-41.

114. Komiyama, T., and L. Luo. 2006. Development of wiring specificity in the olfactory system. Curr Opin Neurobiol 16:67-73.

115. Urbanska, M., M. Blazejczyk, and J. Jaworski. 2008. Molecular basis of dendritic arborization. Acta Neurobiol Exp (Wars) 68:264-288.

116. Pelham, R. J., Jr., and Y. L. Wang. 1998. Cell locomotion and focal adhesions are regulated by the mechanical properties of the substrate. Biol Bull 194:348-349; discussion 349-350.

117. Yamamoto, M., R. Ueda, K. Takahashi, K. Saigo, and T. Uemura. 2006. Control of axonal sprouting and dendrite branching by the Nrg-Ank complex at the neuron-glia interface. Curr Biol 16:1678-1683.

118. Tropea, M., M. I. Johnson, and D. Higgins. 1988. Glial cells promote dendritic development in rat sympathetic neurons in vitro. Glia 1:380-392.

119. Higgins, D., M. Burack, P. Lein, and G. Banker. 1997. Mechanisms of neuronal polarity. Curr Opin Neurobiol 7:599-604.

120. Pierret, P., N. Quenneville, S. Vandaele, R. Abbaszadeh, C. Lanctot, P. Crine, and G. Doucet. 1998. Trophic and tropic effects of striatal astrocytes on cografted mesencephalic dopamine neurons and their axons. J Neurosci Res 51:23-40.

121. Gomes, F. C., T. C. Spohr, R. Martinez, and V. Moura Neto. 2001. Cross-talk between neurons and glia: highlights on soluble factors. Braz J Med Biol Res 34:611-620.

122. Mattson, M. P., P. Dou, and S. B. Kater. 1988. Outgrowth-regulating actions of glutamate in isolated hippocampal pyramidal neurons. J Neurosci 8:2087-2100.

123. Rothstein, J. D., L. Martin, A. I. Levey, M. Dykes-Hoberg, L. Jin, D. Wu, N. Nash, and R. W. Kuncl. 1994. Localization of neuronal and glial glutamate transporters. Neuron 13:713-725.

124. Danbolt, N. C. 2001. Glutamate uptake. Prog Neurobiol 65:1-105.

125. Bhugra, D. 2005. The global prevalence of schizophrenia. PLoS Med 2:e151; quiz e175.

126. Freeman, D. 2008. Studying and treating schizophrenia using virtual reality: a new paradigm. Schizophr Bull 34:605-610.

127. Liddle, P. F. 1987. The symptoms of chronic schizophrenia. A re-examination of the positive-negative dichotomy. Br J Psychiatry 151:145-151.

128. Kuperberg, G., and S. Heckers. 2000. Schizophrenia and cognitive function. Curr Opin Neurobiol 10:205-210.

129. Wratten, N. S., H. Memoli, Y. Huang, A. M. Dulencin, P. G. Matteson, M. A. Cornacchia, M. A. Azaro, J. Messenger, J. E. Hayter, A. S. Bassett, S. Buyske, J. H. Millonig, V. J. Vieland, and L. M. Brzustowicz. 2009. Identification of a schizophrenia-associated functional noncoding variant in NOS1AP. Am J Psychiatry 166:434-441.

130. Brzustowicz, L. M. 2008. NOS1AP in schizophrenia. Curr Psychiatry Rep 10:158-163.

131. Tochio, H., F. Hung, M. Li, D. S. Bredt, and M. Zhang. 2000. Solution structure and backbone dynamics of the second PDZ domain of postsynaptic density-95. J Mol Biol 295:225-237.

132. Ohnuma, T., H. Kato, H. Arai, R. L. Faull, P. J. McKenna, and P. C. Emson. 2000. Gene expression of PSD95 in prefrontal cortex and hippocampus in schizophrenia. Neuroreport 11:3133-3137.

133. Dean, B., A. Digney, S. Sundram, E. Thomas, and E. Scarr. 2008. Plasma apolipoprotein E is decreased in schizophrenia spectrum and bipolar disorder. Psychiatry Res 158:75-78.

134. Senitz, D., and E. Winkelmann. 1981. [Morphology of the orbitofrontal cortex in persons schizophrenic psychotics. A Golgi and electron microscopy study]. Psychiatr Neurol Med Psychol (Leipz) 33:1-9.

135. Senitz, D., and E. Winkelmann. 1991. [Neuronal structure abnormality in the orbito-frontal cortex of schizophrenics]. J Hirnforsch 32:149-158.

136. Thomas, E. A., B. Dean, E. Scarr, D. Copolov, and J. G. Sutcliffe. 2003. Differences in neuroanatomical sites of apoD elevation discriminate between schizophrenia and bipolar disorder. Mol Psychiatry 8:167-175.

137. Mahley, R. W. 1988. Apolipoprotein E: cholesterol transport protein with expanding role in cell biology. Science 240:622-630.

138. Harrington, C. R., J. R. Anderson, and K. K. Chan. 1995. Apolipoprotein E type epsilon 4 allele frequency is not increased in patients with sporadic inclusion-body myositis. Neurosci Lett 183:35-38.

139. Digney, A., D. Keriakous, E. Scarr, E. Thomas, and B. Dean. 2005. Differential changes in apolipoprotein E in schizophrenia and bipolar I disorder. Biol Psychiatry 57:711-715.

140. Gupta, D. S., R. E. McCullumsmith, M. Beneyto, V. Haroutunian, K. L. Davis, and J. H. Meador-Woodruff. 2005. Metabotropic glutamate receptor protein expression in the prefrontal cortex and striatum in schizophrenia. Synapse 57:123-131.

141. Thomann, P. A., M. Roebel, V. Dos Santos, S. Bachmann, M. Essig, and J. Schroder. 2009. Cerebellar substructures and neurological soft signs in first-episode schizophrenia. Psychiatry Res.

142. Thomann, P. A., T. Wustenberg, V. D. Santos, S. Bachmann, M. Essig, and J. Schroder. 2009. Neurological soft signs and brain morphology in first-episode schizophrenia. Psychol Med 39:371-379.

143. Avila, M. T., M. A. Weiler, A. C. Lahti, C. A. Tamminga, and G. K. Thaker. 2002. Effects of ketamine on leading saccades during smooth-pursuit eye movements may implicate cerebellar dysfunction in schizophrenia. Am J Psychiatry 159:1490-1496.

144. Kapoor, R., K. S. Lim, A. Cheng, T. Garrick, and V. Kapoor. 2006. Preliminary evidence for a link between schizophrenia and NMDA-glycine site receptor ligand metabolic enzymes, d-amino acid oxidase (DAAO) and kynurenine aminotransferase-1 (KAT-1). Brain Res 1106:205-210.

145. Wright, I. C., S. Rabe-Hesketh, P. W. Woodruff, A. S. David, R. M. Murray, and E. T. Bullmore. 2000. Meta-analysis of regional brain volumes in schizophrenia. Am J Psychiatry 157:16-25.

146. Beneyto, M., L. V. Kristiansen, A. Oni-Orisan, R. E. McCullumsmith, and J. H. Meador-Woodruff. 2007. Abnormal glutamate receptor expression in the medial temporal lobe in schizophrenia and mood disorders. Neuropsychopharmacology 32:1888-1902.

147. McCarley, R. W., C. G. Wible, M. Frumin, Y. Hirayasu, J. J. Levitt, I. A. Fischer, and M. E. Shenton. 1999. MRI anatomy of schizophrenia. Biol Psychiatry 45:1099-1119.

148. Bogerts, B., M. Ashtari, G. Degreef, J. M. Alvir, R. M. Bilder, and J. A. Lieberman. 1990. Reduced temporal limbic structure volumes on magnetic resonance images in first episode schizophrenia. Psychiatry Res 35:1-13.

149. Hirayasu, Y., M. E. Shenton, D. F. Salisbury, C. C. Dickey, I. A. Fischer, P. Mazzoni, T. Kisler, H. Arakaki, J. S. Kwon, J. E. Anderson, D. Yurgelun-Todd, M. Tohen, and R. W. McCarley. 1998. Lower left temporal lobe MRI volumes in patients with first-episode schizophrenia compared with psychotic patients with first-episode affective disorder and normal subjects. Am J Psychiatry 155:1384-1391.

150. Medoff, D. R., H. H. Holcomb, A. C. Lahti, and C. A. Tamminga. 2001. Probing the human hippocampus using rCBF: contrasts in schizophrenia. Hippocampus 11:543-550.

151. Deicken, R. F., M. Pegues, and D. Amend. 1999. Reduced hippocampal N-acetylaspartate without volume loss in schizophrenia. Schizophr Res 37:217-223.

152. O'Donnell, B. F., J. M. Swearer, L. T. Smith, P. G. Nestor, M. E. Shenton, and R. W. McCarley. 1996. Selective deficits in visual perception and recognition in schizophrenia. Am J Psychiatry 153:687-692.

153. Tek, C., J. Gold, T. Blaxton, C. Wilk, R. P. McMahon, and R. W. Buchanan. 2002. Visual perceptual and working memory impairments in schizophrenia. Arch Gen Psychiatry 59:146-153.

154. Wynn, J. K., M. F. Green, S. Engel, A. Korb, J. Lee, D. Glahn, K. H. Nuechterlein, and M. S. Cohen. 2008. Increased extent of object-selective cortex in schizophrenia. Psychiatry Res 164:97-105.

155. Onitsuka, T., R. W. McCarley, N. Kuroki, C. C. Dickey, M. Kubicki, S. S. Demeo, M. Frumin, R. Kikinis, F. A. Jolesz, and M. E. Shenton. 2007. Occipital lobe gray matter volume in male patients with chronic schizophrenia: A quantitative MRI study. Schizophr Res 92:197-206.

156. Thomas, E. A., B. Dean, G. Pavey, and J. G. Sutcliffe. 2001. Increased CNS levels of apolipoprotein D in schizophrenic and bipolar subjects: implications for the pathophysiology of psychiatric disorders. Proc Natl Acad Sci U S A 98:4066-4071.

157. Preston, A. R., D. Shohamy, C. A. Tamminga, and A. D. Wagner. 2005. Hippocampal function, declarative memory, and schizophrenia: anatomic and functional neuroimaging considerations. Curr Neurol Neurosci Rep 5:249-256.

158. Leshchyns'ka, I., V. Sytnyk, J. S. Morrow, and M. Schachner. 2003. Neural cell adhesion molecule (NCAM) association with PKCbeta2 via betaI spectrin is implicated in NCAM-mediated neurite outgrowth. J Cell Biol 161:625-639.

159. Turner, D. C., L. A. Flier, and S. Carbonetto. 1989. Identification of a cell-surface protein involved in PC12 cell-substratum adhesion and neurite outgrowth on laminin and collagen. J Neurosci 9:3287-3296.

160. Edgar, D. 1989. Neuronal laminin receptors. Trends Neurosci 12:248-251.

161. Sniadecki, N. J., and C. S. Chen. 2007. Microfabricated silicone elastomeric post arrays for measuring traction forces of adherent cells. Methods Cell Biol 83:313-328.

162. Lemmon, C. A., N. J. Sniadecki, S. A. Ruiz, J. L. Tan, L. H. Romer, and C. S. Chen. 2005. Shear force at the cell-matrix interface: enhanced analysis for microfabricated post array detectors. Mech Chem Biosyst 2:1-16.

163. Amara, S. G., and A. C. Fontana. 2002. Excitatory amino acid transporters: keeping up with glutamate. Neurochem Int 41:313-318.

164. Shigeri, Y., R. P. Seal, and K. Shimamoto. 2004. Molecular pharmacology of glutamate transporters, EAATs and VGLUTs. Brain Res Brain Res Rev 45:250-265.

165. Kanner, B. I. 2006. Structure and function of sodium-coupled GABA and glutamate transporters. J Membr Biol 213:89-100.

166. Husi, H., M. A. Ward, J. S. Choudhary, W. P. Blackstock, and S. G. Grant. 2000. Proteomic analysis of NMDA receptor-adhesion protein signaling complexes. Nat Neurosci 3:661-669.

167. Saglietti, L., C. Dequidt, K. Kamieniarz, M. C. Rousset, P. Valnegri, O. Thoumine, F. Beretta, L. Fagni, D. Choquet, C. Sala, M. Sheng, and M. Passafaro. 2007. Extracellular interactions between GluR2 and N-cadherin in spine regulation. Neuron 54:461-477.

168. Nuriya, M., and R. L. Huganir. 2006. Regulation of AMPA receptor trafficking by N-cadherin. J Neurochem 97:652-661.

169. Kruse, S. A., G. H. Rose, K. J. Glaser, A. Manduca, J. P. Felmlee, C. R. Jack, Jr., and R. L. Ehman. 2008. Magnetic resonance elastography of the brain. Neuroimage 39:231-237.

170. Miller, K. 2000. Biomechanics of soft tissues. Med Sci Monit 6:158-167.

171. Robertson, C. S., R. K. Narayan, C. F. Contant, R. G. Grossman, Z. L. Gokaslan, R. Pahwa, P. Caram, Jr., R. S. Bray, Jr., and A. M. Sherwood. 1989. Clinical

experience with a continuous monitor of intracranial compliance. J Neurosurg 71:673-680.

CURRICULUM VITAE

Michelle L. Previtera

Education

9/2001-5/2003	Rutgers University, The State University of New Jersey, Camden. Biotechnology. No degree earned.
9/2003-5/2005	Thomas Jefferson University. Biotechnology. B.S.
9/2005-present	Rutgers University, The State University of New Jersey, New Brunswick. Molecular Biosciences. Ph.D.

Principle Occupation

2005-present	UMDNJ/Rutgers Graduate Student
2006-2008	IGERT Rutgers Program on Integratively Engineered Biointerfaces Fellow
2008-2009	Rutgers Louis Bevier Graduate Dissertation Fellow

Publications

Jiang, X., P. C. Georges, B. Li, Y. Du, M. K. Kutzing, M. L. Previtera, N. A. Langrana, and B. L. Firestein. 2007. Cell Growth in Response to Mechanical Stiffness is Affected by Neuron-Astroglia Interactions. The Open Neuroscience Journal 1:7-14.

Previtera, M.P. C.G, Langhammer, B.L. Firestein. Substrate stiffness affects the dendrite patterning of hippocampal neurons independent of cell density. Cellular and Molecular Bioengineering, In review.

Previtera, M.P. C.G, Langhammer, N.A. Langrana, B.L. Firestein. Regulation of dendrite arborization by substrate stiffness is mediated by glutamate receptors. Submitted.